

Sophie Seehuus Berg

Real-Time Parameter Identification for Reliable Operation of Synchronous Generators

Master's thesis in Energy and Environmental Engineering

Supervisor: Jonas Nøland

June 2020

Abstract

This master thesis explores the online identification methods for synchronous machine parameters using online measurements. The central concept of the online parameter estimation algorithm is to use the dynamic measurements from the machine in combination with the manufacturer's estimates of the parameters to make the machine model agree with the measurements. The goal is to use already available measurements to improve upon manufacturers estimates of the synchronous machine parameters which may be obtained from stand-still tests decades ago.

The model of the generator is based on Park's model of the synchronous machine with an observer for the damper winding currents. The generator modelled was a ten pole salient-pole synchronous generator from Voith situated in a German hydropower-plant. Three hundred seconds of voltage and current measurements was received from the generator during steady-state running on rated load connected to the grid. Inductances and resistances of the generator were calculated from the available data from the datasheet. The model for the parameter estimation is built in MATLAB Simulink. To estimate the rotor position of the generator, a phase-locked-loop control system was implemented on the signal from the phase a voltage. A Kalman Filter was used as an optimal observer to filter and correct the measurements by using previous knowledge about the synchronous generator and its parameters. The method for parameter estimation uses the recursive least squares (RLS) algorithm to create an estimate for the inductances and resistances of the machine using available measurements.

However, due to disturbances and noise present in the measurements of the field voltage and current, results from the parameter estimation using the real measurements from the generator had large errors. For this reason, it was decided to use measurements created by a Synchronous Machine block from the Simscape library in Simulink which was modelled to be equal to the Voith generator for further simulations. To explore how the algorithm reacts to changes in the machine parameters, a case study is presented where the RLS algorithm was given a deliberately faulty initial estimate for the parameter estimation. The algorithm first showed poor ability to track changes in the machine parameters and would converge towards an erroneous estimate. However, after tuning of the initial parameter covariance matrix, the parameter estimation showed significant improvements. It was able to converge towards the correct value of the parameter even with an incorrect initial estimate. The conjecture from the thesis is that the parameter estimation algorithm, if tuned correctly, could give more accurate estimations for the parameters of the ma-

chine, than the manufacturer's parameters obtained from stand-still tests possibly from many years ago. However, before the algorithm could be used in the industry a more effective way for noise filtering and rejection of bad measurements has to be implemented.

Sammendrag

Denne masteroppgaven utforsker metoder for online identifisering av synkronmaskiner ved hjelp av online målinger. Det sentrale konseptet for online parameterestimeringsalgoritmen er å bruke de dynamiske målingene fra maskinen i kombinasjon med estimater av parametrene for å få maskinmodellen til å stemme overens med målingene. Målet er å bruke allerede tilgjengelige målinger for å forbedre produsentens estimater av synkronmaskinparametrene som muligens er kalkulert fra still-still-tester for flere tiår siden.

Modellen av generatoren er basert på Parks modell av synkronmaskiner med en observatør for demperviklingsstrømmene. Generatoren som ble modellert var en ti-pol salient-pole synkrongenerator fra Voith som ligger i et tysk vannkraftverk. Tre hundre sekunder spennings- og strømmålinger ble mottatt fra generatoren under steady-state med nominell last koblet til nettet. Induktanser og motstander til generatoren ble beregnet ut fra tilgjengelige data fra databladet. Modellen for parameterestimering er bygget i MATLAB Simulink. For å estimere rotorposisjonen til generatoren, ble benyttet et phase-locked-loop kontrollsystem signalet fra fasespenningen til fase a. Et Kalman-filter ble brukt som en optimal observatør for å filtrere og korrigere målingene ved å bruke tidligere kunnskap om generatoren og dens parametre. Metoden for parameterestimering bruker recursive least squares (RLS) algoritmen for å lage et estimat for induktansene og motstandene til maskinen ved å bruke tilgjengelige målinger.

På grunn av forstyrrelser og støy tilstede i målingene av feltspenning og -strøm, ga imidlertid resultater fra parameterestimeringen ved bruk av de virkelige målingene fra generatoren store feil. Av denne grunn ble det besluttet å bruke målinger opprettet av en Synchronous Machine-blokk fra Simscape-biblioteket i Simulink som ble modellert til å være lik Voith-generatoren for videre simuleringer. For å utforske hvordan algoritmen reagerer på endringer i maskinparametrene, presenteres en casestudie der RLS-algoritmen ble gitt et feil initialt estimat for parameterestimering. Algoritmen viste først dårlig evne til å spore endringer i maskinparametrene og konvergente mot et feilaktig estimat. Imidlertid, etter tuning av intiell parameter-kovariansmatrise, viste parameterestimeringen betydelige forbedringer. Den var i stand til å konvergere mot riktig verdi av parameteren selv med et feil initialt estimat. Konklusjonen fra oppgaven er at parameterestimeringsalgoritmen, hvis den er tunet riktig, kan gi mer nøyaktige estimater for maskinens parametre enn produsentens parametre hentet fra 'stand-still'-tester muligens fra mange år siden. Før algoritmen kan brukes i bransjen, må det imidlertid implementeres en mer effektiv måte for støyfiltrering og avvising av dårlige målinger.

Preface

This master's thesis was written during the spring semester of 2020 at the Department of Electric Power Engineering at the Norwegian University of Science and Technology. The thesis completes the degree Master of Science in the study program Energy and Environmental Engineering. The thesis is written in cooperation with HydroCen and Hymatek.

The topic of this thesis has been interesting, and it has been exciting working with something that is both highly relevant for my future job and forward-looking. The synchronous generator has been studied for decades and is still relevant, and it will probably stay that way in the unforeseen future. I could have studied the synchronous generator for multiple years and still not fully understand it and keep up with all new research.

The semester which I wrote my masters will be memorable for many different reasons, but the dominant factor is the coronavirus. Like many others, all my plans were cancelled, and my reality was flipped on the head. As I write this, I am sitting at my desk in my bedroom where I have spent too many hours. Homeoffice has been challenging, and motivation was not always as easy to come by. I did not know it was possible to miss the campus and my desk at our reading room. I forgot how spoiled we were to have our supervisors in an office just meters from where I worked. Nonetheless, I have begun to appreciate different things. I also am hugely grateful to my supervisor, Jonas Nøland, and my co-supervisor, Erick Alves, that have been extremely available and I am thankful that a video call on teams can be of as low threshold as stopping by the office.

I am also deeply grateful for my fellow students, especially Mona, Nina, Ulrikke and Mathilde, your company for hundreds of lunches has been appreciated.

Lastly, I would like to thank my friends and colleges of Kulturutvalget at Studentersamfundet i Trondhjem; the last years would not have been as fun without all of you.

Trondheim, 2020-04-06

Sophie Seehus Berg

Table of Contents

Abstract	i
Sammendrag	ii
Preface	iii
Table of Contents	vi
List of Tables	viii
List of Figures	x
1 Introduction	1
1.1 Background	1
1.2 Previous Work	2
1.3 Problem Definition	2
1.4 Related Work	2
1.5 Thesis Outline	4
2 Basic Theory	5
2.1 Synchronous Machines	5
2.1.1 Flux linkages in stator reference frame	7
2.1.2 Flux Linkages in Rotor Reference Frame	8
2.1.3 Voltage Equations	10
2.1.4 Rotor angle position	12
2.2 Per unit system	12

2.2.1	Stator Base Quantities	13
2.2.2	Rotor base quantities	14
2.2.3	Synchronous Machine Parameters	18
2.3	Noise filtering	21
2.3.1	Kalman Filter	22
2.4	Recursive Least Squares algorithm	24
2.4.1	Recursive Least Squares Parameter Equations	24
3	Method and model	27
3.1	Creation of a State-Space Representation	27
3.2	Observer for damper winding currents	29
3.3	Calculate Parameters of the Synchronous Generator	29
3.4	Simulink Model	32
3.4.1	Testing Parameter Estimation using real data	32
4	Results	36
4.1	Specifications of Machine	36
4.2	Parameter Estimation with Real Measurements	38
4.2.1	Parameter Estimation with Damper Winding Currents Set to Zero	42
4.3	Back to the "Synchronous Machine"-block	44
4.3.1	Sensitivity analysis	45
4.3.1.1	Case 1: Basecase: $\hat{\theta}_0 = \theta$	46
4.3.1.2	Case 2: $\hat{\theta}_0 = 0.95 \theta$	47
4.3.1.3	Case 3: $\hat{\theta}_0 = 1.05 \theta$	49
4.3.1.4	Case 4: $\hat{\theta}_0 = 0.90 \theta$	51
4.3.1.5	Case 5: $\hat{\theta}_0 = 1.1 \theta$	52
4.4	Tuning of Algorithm	53
4.4.1	Tuning of Forgetting Factor, λ	53
4.4.2	Tuning of the Initial Parameter Covariance Matrix	54
5	Discussion	57
5.1	Results using real data	57
5.1.1	Leakage inductance	58
5.2	Sensitivity analysis	58
5.2.1	Tuning of algorithm	58
6	Conclusion and Future Work	60
6.1	Summary and Conclusion	60

6.2 Future Work	62
Bibliography	62

List of Tables

2.1	Stator base quantities, Kundur	14
2.2	Stator base quantities, thesis model	14
2.3	Rotor base quantities, Kundur	15
2.4	Rotor base quantities, thesis	17
2.5	Notation for the synchronous machine parameters used in this thesis . . .	20
2.6	Notation for RLS parameters used in thesis	26
4.1	Machine rated data of the Voith salient-pole synchronous generator	36
4.2	Standard Parameters for the Voith synchronous generator from datasheet .	37
4.3	Calculated Parameters	38
4.4	Error deviation given in % from datasheet values for the parameter estimation from RLS after 30 seconds of simulation. Data from real measurements from generator during rated load, and damper winding currents set to zero.	43
4.5	Estimations of Standard Parameters given in % from datasheet values. Calculated from the estimated parameters from RLS, after 30 seconds of simulations, using measurements from real generator during rated load with damper winding currents assumed zero.	44
4.6	Error given in % of the estimated standard parameters compared to datasheet values. Standard parameters are calculated using the estimated parameters from the RLS-algorithm with $\hat{\theta}_0 = \theta$. Measurements from "Synchronous Machine"-block running on rated load during steady-state. . . .	47

4.7	Error given in % of the estimated standard parameters compared to datasheet values. Standard parameters are calculated using the estimated parameters from the RLS-algorithm with $\hat{\theta}_0 = 0.95 \theta$. Measurements from "Synchronous Machine"-block running on rated load during steady-state. . . .	49
4.8	Error given in % of the estimated standard parameters for Case 3: $\hat{\theta}_0 = 1.05 \theta$	50
4.9	Error given in % of the estimated standard parameters for Case 4: $\hat{\theta}_0 = 0.9 \theta$	51
4.10	Error given in % of the estimated standard parameters for Case 5: $\hat{\theta}_0 = 1.1 \theta$	52
4.11	Standard Parameter estimation with 10% larger parameters.	55

List of Figures

2.1	Schematic diagram of a three-phase two pole synchronous machine and the circuits for the axes [1].	6
2.2	The sets of fictitious dq0-windings representing the three-phase stator windings. [1].	10
2.3	Equivalent circuit commonly used for synchronous machines	19
2.4	The Kalman filter loop.	23
3.1	Simulink model using real measurements from a synchronous generator	33
4.1	Sample of the field voltage of the Voith generator during rated load in per unit showing the noise of the signal	39
4.2	Sample of the observed d-axis damper winding current of the Voith generator during rated load. Showing the signal is clearly affected by noise.	40
4.3	First ten seconds of the parameter estimation from the RLS-block by using noisy measurements from a real generator at rated load.	41
4.4	First ten seconds of error in parameter estimations from the RLS-block of estimating the parameters of the synchronous generator using data from real measurements while damper winding currents set to zero.	42
4.5	Errors of the parameter estimation for the basecase with $\hat{\theta}_0 = \theta$ in the RLS algorithm. Measurements from "Synchronous Machine"-block running on rated load during steady-state.	46
4.6	Errors of the parameter estimation for the basecase with $\hat{\theta}_0 = 0.95\theta$ in the RLS algorithm. Measurements from "Synchronous Machine"-block running on rated load during steady-state.	48

4.7	Errors of the parameter estimation for the basecase with $\hat{\theta}_0 = 1.05\theta$ in the RLS algorithm. Measurements from "Synchronous Machine"-block running on rated load during steady-state.	50
4.8	Errors of the parameter estimation for the case 4 with $\hat{\theta}_0 = 0.9\theta$ in the RLS algorithm. Measurements from "Synchronous Machine"-block running on rated load during steady-state.	51
4.9	Errors of the parameter estimation for the case 4 with $\hat{\theta}_0 = 1.1\theta$ in the RLS algorithm. Measurements from "Synchronous Machine"-block running on rated load during steady-state.	52
4.10	Errors of the parameter estimation after tuning P_0 with $\hat{\theta}_0 = 1.1\theta$ in the RLS algorithm. Measurements from "Synchronous Machine"-block running on rated load during steady-state.	55
4.11	Errors of the parameter estimation of L_{ad} after tuning P_0 with $\hat{\theta}_0 = 1.1\theta$ in the RLS algorithm. Measurements from "Synchronous Machine"-block running on rated load during steady-state.	56

Introduction

1.1 Background

Global increase in the utilization of renewable energy has a significant impact on the operating regimes of conventional power plants. Synchronous generators are the bulk of power generation worldwide and form the principal source of electric energy in power systems. In Norway, 95% of the electricity production comes from hydropower [2] where the use of salient-pole synchronous generators are the norm. Therefore, the proper understanding of these devices is essential for planning, operation, and control of the power system. The information about the synchronous generator parameters is important for both reliable stability studies and "post mortem" analyses [3].

A valid model for synchronous generators is essential for a valid analysis of stability and dynamic performance [4]. Today the machine parameters are calculated only in the design phase during standstill frequency measurements by the manufactures. Offline parameter estimation methods are both expensive and inconvenient as it leads to loss of income for power producers. Also, offline identification of the parameters is often inaccurate as many parameters change with different levels of excitation and loading, and saturation. Online parameter estimation is therefore attractive, as it can be more accurate and have no interference for the regular operation of the machine. In addition, the continuous tracking of parameters values over time enables power generation companies to foresee generator failures, such as turn-to-turn short circuits in the field winding and rotor imbalance. Accordingly, it is possible to avoid outages and save large amounts of

resources due to rehabilitation of the machine, loss of income and social costs. A goal for this master thesis will attempt to solve a well-defined problem for the industry; the identification of synchronous generator parameters and the tracking of parameters over time to potentially prevent system outages.

1.2 Previous Work

This master thesis is a continuation of the work performed in the pre-master project last fall [5] and the work performed by Erick F.Alves in his master thesis, [6]. In [6], a MATLAB Simulink model was created for estimation of synchronous machine parameters based on estimating the impedance shape of the synchronous machine under operation. His thesis proved that 8 out of 13 parameters could be reliably estimated with the use of a Kalman Filter and the Recursive Least Squares algorithm. The main focus of the fall's pre-master project was to explore if the parameter estimation performed in [6] could be improved by including the saturation effect in the model of the synchronous generator. However, the results showed that there were no improvements in the parameter estimations of the machine after the saturation effect is included.

1.3 Problem Definition

This master's thesis further delve into the theory of the synchronous machine and the aspects of parameter estimation. There were multiple ways to continue the work performed in the fall, but it was chosen to test if the parameter estimation algorithm created in [6] could be validated using data from measurements from a real hydropower-plant. The data available to validate the algorithm was high-frequency data from a Voith salient-pole synchronous generator situated in a German hydropower-plant. Before the algorithm could be tested, a model of the synchronous generator had to be created, and the electrical parameters had to be calculated. In addition, it was decided to examine the performance of the estimation algorithm with reduced knowledge of the parameters. Another goal of this thesis is to achieve a good and thorough understanding and knowledge about all aspects of the parameter estimation.

1.4 Related Work

Sherwin Wright wrote in 1931: "The importance of the analysis of synchronous machine operation is well evidenced by the considerable literature on this subject, representing

definite steps in the advancement of the art' [7]. Almost one hundred years later, the literature on the synchronous machine has considerably grown, and the subject is far from dated. It might even have gotten more relevant, as with increasing complexities in power systems, more accurate models and parameters of subsystems, particularly synchronous generators have become essential [8]. The main initial advance in the modelling of synchronous machines was with the development of Park's model, in 1929 with [9]. Park's model for the synchronous machine is standard practice to use for all engineering applications, and will also be used for this thesis. However, to use this model multiple resistances and inductances for the machines needs to be known. The different methods for synchronous machine parameter estimation can be summed up by analysis of transient data (short-circuit tests or load rejections) or frequency response tests, with disturbances in standstill, offline or online operations [10]. The literature in the field of online synchronous machine parameters estimation is steadily growing. However, the conventional method of determining parameters through offline tests through open- and short-circuit tests on unloaded machines is still the most used. There are many limitations to these tests which have been recognized for decades, so better models are continuously researched.

The alternative to offline parameter identification methods is parameter estimation using measurements with the machine is running and carrying a load, referred to as online parameter identification. The main attraction of online methods is their minimal interference with the normal operation of the generator. Many different algorithms are used for this and have been proven to give accurate estimations of the machine parameters. One of the more common algorithms is different versions of the least-squares estimators. The least-squares algorithm is applied by, among others, [10–14]. Another popular algorithm is the maximum likelihood method which is used to perform parameter estimations in [14–16]. The methods of parameter identification are varied, but the approaches can be summarized with the measured outputs of voltage and currents being used for identification of parameters by an estimator.

1.5 Thesis Outline

- Chapter 2 introduces the basic theory about the synchronous machine, the Kalman Filter, and the Recursive Squares algorithm.
- Chapter 3 presents how the state-space representation of the synchronous model is created, and details about the observer for the damper winding currents. After this, it is explained how the electrical parameters of the synchronous machine from values collected from the datasheet. The Simulink model used in the thesis is also presented in this chapter.
- Chapter 4 first presents the specifications of the machine used for this thesis. After this the results from the parameter estimation using the real measurements is showed. A case study to explore how the RLS algorithm handle errors in the initial estimation of the parameter is also presented. Lastly results achieved after the RLS algorithm is tuned is given.
- Chapter 5 includes the discussion of the method and results.
- Chapter 6 presents the conclusion of the thesis and some thoughts on further work.

Basic Theory

2.1 Synchronous Machines

Before a parameter estimation can be performed, a good and thorough knowledge of the general synchronous machine is needed. A state-space formulation of the synchronous machine is necessary. There is a vast amount of literature that deals with synchronous machine theory, but the mathematical model of the synchronous generator which is presented here is based on the theory from [1], and the notation follows the IEEE convention.

The synchronous generator consists of two magnetic parts; rotor and stator, where the stator is connected to the grid. The generator is supplied with fixed voltages and frequency from the grid. By definition, the synchronous generator produces electricity with a frequency synchronized with the mechanical rotational speed [17]. The simplest version of a synchronous generator has two poles, one south and one north pole. However, low-speed generators, such as the ones used for hydropower turbines, often have many poles. With multiple field pole pairs, each passing of a south and north pole completes a cycle of a magnet field oscillation. The stator windings will also be made of multiple corresponding sets of coils as the number of field poles. The relationship between the rotor angle expressed in electrical units and mechanical units is shown by eq. (2.1).

$$\theta_{elec} = p \cdot \theta_{mech} \tag{2.1}$$

Where p is the number of pole pairs, θ_{elec} is the electrical angle, and θ_{mech} is the corresponding mechanical angle.

These magnetic poles can either be of the salient or nonsalient type, where the salient poles are protruding. The salient-pole rotor introduces a non-uniformity of the magnetic reluctance of the air gap [18]. This type of synchronous machines is often used for low-speed generators where it is beneficial to have many pole pairs, as the synchronous speed of the machine is given by eq. (2.2).

$$n = \frac{240f}{p} \tag{2.2}$$

The generic mathematical model of a synchronous machine has three stator windings, one field winding and two amortisseur or damper windings. These six windings are magnetically coupled as a function of the rotor position. The cross-section of such a machine is pictured in fig. 2.1.

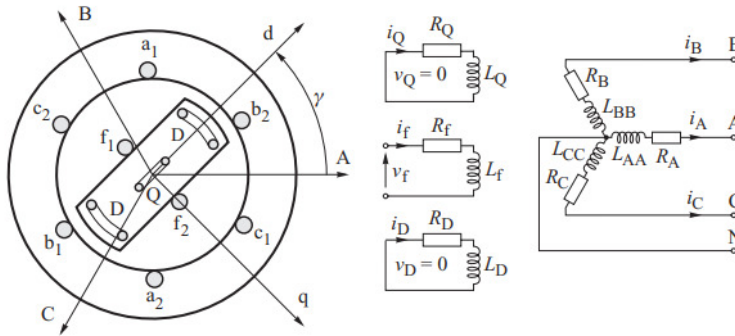


Figure 2.1: Schematic diagram of a three-phase two pole synchronous machine and the circuits for the axes [1].

The field winding (f_1, f_2) carries the direct current which produces a magnetic field that in return induces three-phase alternating voltages in the armature windings ($a_1, a_2, b_1, b_2, c_1, c_2$). The stator windings carry the load current which supplies power to the system. In addition, the generator has two damper windings which are short-circuited; one on the direct-axis (D) and another on the quadrature-axis (Q). In fig. 2.1 the d-axis is centred magnetically in the centre of the north pole and q-axis 90 electrical degrees ahead of the d-axis. The choice of the q-axis leading the d-axis is arbitrary, and it might as well be the other way around.

Before the mathematical model of the synchronous machine can be created, it is convenient to make some assumptions, which are as follows:

1. The stator windings are symmetrical.
2. The capacitance of the windings can be neglected.
3. The originally distributed windings can be represented on the form of a concentrated winding.
4. The change in the inductance of the stator windings due to rotor position is sinusoidal and does not contain higher harmonics.
5. Hysteresis loss is negligible, but the influence of eddy currents can be included in the model of the damper windings.
6. In the transient and subtransient states, the rotor speed is near synchronous speed.
7. The magnetic circuits are linear (not saturated), and the inductance values do not depend on the current.

2.1.1 Flux linkages in stator reference frame

The windings are magnetically coupled, so the flux in the separate windings are dependent on the current in all the other windings. This fact is represented by the following matrix equation in eq. (2.3).

$$\begin{array}{c} \text{Stator} \\ \text{Rotor} \end{array} \left\{ \begin{array}{l} \Psi_A \\ \Psi_B \\ \Psi_C \\ \Psi_f \\ \Psi_D \\ \Psi_Q \end{array} \right\} = \begin{array}{c} \left[\begin{array}{ccc|ccc} L_{AA} & L_{AB} & L_{AC} & L_{Af} & L_{AD} & L_{AQ} \\ L_{BA} & L_{BB} & L_{BC} & L_{Bf} & L_{BD} & L_{BQ} \\ L_{CA} & L_{CB} & L_{CC} & L_{Cf} & L_{CD} & L_{CQ} \\ \hline L_{fA} & L_{fB} & L_{fC} & L_{ff} & l_f & L_{fQ} \\ L_{DA} & L_{DB} & L_{DC} & L_{Df} & L_{DD} & L_{DQ} \\ L_{QA} & L_{QB} & L_{QC} & L_{Qf} & L_{QD} & L_{QQ} \end{array} \right] \begin{array}{l} i_A \\ i_B \\ i_C \\ i_f \\ i_D \\ i_Q \end{array} \right. \quad (2.3)
 \end{array}$$

Equation (2.3) shows how the inductances represent the proportionality between a flux linkage and a current. In this form, the inductances are used as parameters.

The matrix equation can also be written in its compressed form:

$$\begin{bmatrix} \Psi_{ABC} \\ \Psi_{fDQ} \end{bmatrix} = \begin{bmatrix} \mathbf{L}_S & \mathbf{L}_{SR} \\ \mathbf{L}_{SR}^T & \mathbf{L}_R \end{bmatrix} \begin{bmatrix} \mathbf{i}_{ABC} \\ \mathbf{i}_{fDQ} \end{bmatrix} \quad (2.4)$$

Where \mathbf{L}_S , \mathbf{L}_R , \mathbf{L}_{SR} is the matrices of stator self- and mutual inductances, rotor self-and mutual inductances and rotor to stator mutual inductances, respectively. Most of these inductances are dependent on the rotor position and therefore vary with time.

2.1.2 Flux Linkages in Rotor Reference Frame

When viewing the flux linkages in a stator reference frame, one gets the unfortunate occurrence of the inductances not being constant, but varying with time. It is more convenient to transfer the equations into a rotor reference frame, where the reference frame rotates with the rotor. This is more commonly called the Park transformation and was introduced by Robert H. Park in 1929 with [9]. The theories presented in [9] is based on Blondel, Dreyfus, Doherty and Nickles previous work in [19] and [20]. Park's transformation is considered a large breakthrough in the modelling of synchronous machines as it significantly simplifies the analysis of the machine, and almost all analytical models are later based upon this transformation [21].

The Park transformation is performed by transforming the armature currents, voltages and fluxes into two sets of variables in a rotor reference frame, by the using trigonometric functions of the rotor angle, θ . One set is aligned with the magnetic axis of the field winding, also called the direct axis and a second one which is aligned along with the rotor, the rotor quadrature axis. The most fortunate consequence of this transformation is that all the elements of the inductance matrix will be constant and independent of time.

The transformation is defined by the matrix equation given in eq. (2.5).

$$\begin{bmatrix} i_d \\ i_q \\ i_0 \end{bmatrix} = \begin{bmatrix} \beta_d \cos \gamma & \beta_d \cos(\gamma - \frac{2}{3}\pi) & \beta_d \cos(\gamma + \frac{2}{3}\pi) \\ \beta_q \cos \gamma & \beta_q \cos(\gamma - \frac{2}{3}\pi) & \beta_q \cos(\gamma + \frac{2}{3}\pi) \\ \beta_0 & \beta_0 & \beta_0 \end{bmatrix} \begin{bmatrix} i_A \\ i_B \\ i_C \end{bmatrix} \text{ or } \mathbf{i}_{dq0} = \mathbf{W}\mathbf{i}_{ABC} \quad (2.5)$$

Where the coefficients, β_0 , β_d and β_q , are arbitrary non-zero coefficients and introduced due to the change in the reference frame. γ is the rotor angle. The supplement of i_0 is conveniently added to make the transformation unique.

A similar transformation can also be done for the flux linkages and voltages, and this is shown on its compressed form in eq. (2.6).

$$v_{dq0} = \mathbf{W}\mathbf{v}_{ABC} \quad \text{and} \quad \Psi_{dq0} = \mathbf{W}\Psi_{ABC} \quad (2.6)$$

This transformation is not necessary for the rotor currents, voltages and flux linkages as they already are in the rotor reference frame.

The coefficients can be chosen arbitrary, but are usually chosen to be either all equal to $\sqrt{2/3}$ or $2/3$. Both these have their attractions and disadvantages. By choosing $\beta_0 = \frac{1}{\sqrt{3}}$ and $\beta_d = \beta_q = \sqrt{\frac{2}{3}}$ as in [1] and [22], the transformation will be orthogonal and power invariant. However, this has little physical meaning and gives that the equivalent d- and q-axis coils have $\sqrt{3/2}$ times the number of turns as the abc-coils [23]. For this reason [23] chooses the coefficients equal to $2/3$, as this leads to a system which reflects most closely the physical features of the machine.

The coefficients for this thesis model are chosen to be equal to $\sqrt{2/3}$ such that $\mathbf{W}^{-1}=\mathbf{W}^T$ and the transformation power invariant. This orthogonal transformation was proposed in 1951 by Charles Concordia in [22]. The transformation matrix, \mathbf{W} , will then be defined as in eq. (2.7).

$$\mathbf{W} = \sqrt{\frac{2}{3}} \begin{bmatrix} \cos\gamma & \cos(\gamma - \frac{2\pi}{3}) & \cos(\gamma + \frac{2\pi}{3}) \\ \sin\gamma & \sin(\gamma - \frac{2\pi}{3}) & \sin(\gamma + \frac{2\pi}{3}) \\ \frac{1}{\sqrt{2}} & \frac{1}{\sqrt{2}} & \frac{1}{\sqrt{2}} \end{bmatrix} \quad (2.7)$$

This transformation matrix can then be used to transform the matrix equation eq. (2.3) into:

$$\begin{bmatrix} \Psi_d \\ \Psi_q \\ \Psi_0 \\ \Psi_f \\ \Psi_D \\ \Psi_Q \end{bmatrix} = \begin{bmatrix} L_d & & & kM_f & kM_D & \\ & L_q & & & & kM_Q \\ & & L_0 & & & \\ \hline kM_f & & & L_f & l_f & \\ kM_D & & & L_{Df} & L_D & \\ & kM_Q & & & & L_Q \end{bmatrix} \begin{bmatrix} i_d \\ i_q \\ i_0 \\ i_f \\ i_D \\ i_Q \end{bmatrix} \quad (2.8)$$

where $k=\sqrt{3/2}$. When saturation of the iron is neglected, all of the inductances are constant and independent of time as wanted.

By observation of eq. (2.8), it can be seen that there are three independent sets of equations. These three sets of equations are shown in eq. (2.9), (2.10) and (2.11).

$$\Psi_0 = L_0 i_0 \quad (2.9)$$

$$\begin{bmatrix} \Psi_d \\ \Psi_f \\ \Psi_D \end{bmatrix} = \begin{bmatrix} L_d & kM_f & kM_D \\ kM_f & L_f & l_f \\ kM_D & l_f & L_D \end{bmatrix} \begin{bmatrix} i_d \\ i_f \\ i_D \end{bmatrix} \quad (2.10)$$

$$\begin{bmatrix} \Psi_q \\ \Psi_Q \end{bmatrix} = \begin{bmatrix} L_q & kM_Q \\ kM_Q & L_Q \end{bmatrix} \begin{bmatrix} i_q \\ i_Q \end{bmatrix} \quad (2.11)$$

This set of equations together represents the fictitious and uncoupled dq0-windings of the three-phase stator windings and are illustrated in fig. 2.2.

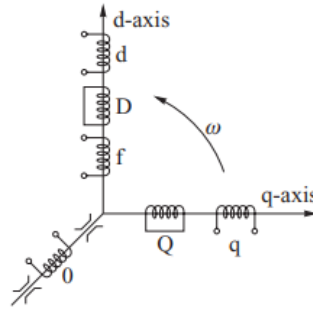


Figure 2.2: The sets of fictitious dq0-windings representing the three-phase stator windings. [1].

In fig. 2.2, does the f correspond to the field winding and D- and Q- corresponds to the damper windings.

2.1.3 Voltage Equations

By applying Kirchoff's voltage law, the voltage equation of the machine in the stator reference frame can be written as:

$$\begin{bmatrix} v_A \\ v_B \\ v_C \\ -v_f \\ 0 \\ 0 \end{bmatrix} \begin{bmatrix} R_A & & & & & \\ & R_B & & & & \\ & & R_C & & & \\ \hline & & & R_f & & \\ & & & & R_D & \\ & & & & & R_Q \end{bmatrix} \begin{bmatrix} i_A \\ i_B \\ i_C \\ i_f \\ i_D \\ i_Q \end{bmatrix} - \frac{d}{dt} \begin{bmatrix} \Psi_A \\ \Psi_B \\ \Psi_C \\ \Psi_f \\ \Psi_D \\ \Psi_Q \end{bmatrix}$$

Or in the compact form:

$$\begin{bmatrix} \mathbf{v}_{ABC} \\ \mathbf{v}_{fDQ} \end{bmatrix} = \begin{bmatrix} \mathbf{R}_{ABC} & \text{---} \\ \text{---} & \mathbf{R}_{fDQ} \end{bmatrix} \begin{bmatrix} \mathbf{i}_{ABC} \\ \mathbf{i}_{fDQ} \end{bmatrix} - \frac{d}{dt} \begin{bmatrix} \Psi_{ABC} \\ \Psi_{fDQ} \end{bmatrix}$$

The voltage equations in the rotor reference frame can be written as:

$$\begin{bmatrix} \mathbf{v}_{dq0} \\ \mathbf{v}_{fDQ} \end{bmatrix} = - \begin{bmatrix} \mathbf{W} & \\ & \mathbf{1} \end{bmatrix} \begin{bmatrix} \mathbf{R}_{ABC} & \\ & \mathbf{R}_{fDQ} \end{bmatrix} \begin{bmatrix} \mathbf{W}^{-1} & \\ & \mathbf{1} \end{bmatrix} \begin{bmatrix} \mathbf{i}_{dq0} \\ \mathbf{i}_{fDQ} \end{bmatrix} \begin{bmatrix} \mathbf{W} & \\ & \mathbf{1} \end{bmatrix} - \frac{d}{dt} \left\{ \begin{bmatrix} \mathbf{W}^{-1} & \\ & \mathbf{1} \end{bmatrix} \begin{bmatrix} \Psi_{dq0} \\ \Psi_{fDQ} \end{bmatrix} \right\} \quad (2.12)$$

When assuming that the resistances in the three phases of the stator is equal, then:

$$\mathbf{W} \mathbf{R}_{ABC} \mathbf{W}^{-1} = R_{ABC} \quad (2.13)$$

It is convenient to define the rotation matrix, Ω , as written in eq. (2.14). This matrix is called the rotation matrix as it introduces terms dependent on the speed of rotation.

$$\Omega = \dot{\mathbf{W}} \mathbf{W} = \omega \begin{bmatrix} 0 & 0 & -1 \\ 0 & 1 & 0 \\ 0 & 0 & 0 \end{bmatrix} \quad (2.14)$$

Equation (2.12) can then be rewritten as:

$$\begin{bmatrix} \mathbf{v}_{dq0} \\ \mathbf{v}_{fDQ} \end{bmatrix} = - \begin{bmatrix} \mathbf{R}_{ABC} & \\ & \mathbf{R}_{fDQ} \end{bmatrix} \begin{bmatrix} \mathbf{i}_{dq0} \\ \mathbf{i}_{fDQ} \end{bmatrix} - \begin{bmatrix} \dot{\Psi}_{dq0} \\ \dot{\Psi}_{fDQ} \end{bmatrix} \begin{bmatrix} \mathbf{W}^{-1} & \\ & \mathbf{1} \end{bmatrix} \begin{bmatrix} \Psi_{dq0} \\ \Psi_{fDQ} \end{bmatrix} \quad (2.15)$$

Where the rotational term, $\Omega \Psi_{0dq}$, represents the EMFs induced in the stator windings due to the rotation of the magnetic field. $\dot{\Psi}$, called the transformer emfs, is the term caused by the changing currents in the coils on the same axis as the ones considered. For the purpose of creating a state-space representation of the synchronous machine, it is desirable to have the voltages expressed in terms of currents only, as the measurements of flux linkages are not available. In addition, the machine is often grounded through an impedance Z_N to limit the zero-sequence current [18].

When substituting the flux linkages for currents and the addition of Z_N , eq. (2.15) can be written as:

$$\begin{bmatrix} v_d \\ v_q \\ v_0 \\ v_f \\ 0 \\ 0 \end{bmatrix} = - \begin{bmatrix} R & \omega L_q & & & & \omega kM_Q \\ -\omega L_d & R & & -\omega kM_f & -\omega kM_D & \\ & & R + 3R_N & & & \\ & & & R_f & & \\ & & & & R_D & \\ & & & & & R_Q \end{bmatrix} \begin{bmatrix} i_d \\ i_q \\ i_0 \\ i_f \\ i_D \\ i_Q \end{bmatrix} \\
 - \frac{d}{dt} \begin{bmatrix} L_d & & & kM_f & kM_D & \\ & L_q & & & & kM_Q \\ & & L_0 + 3L_N & & & \\ & kM_f & & L_f & l_f & \\ & kM_D & & L_{Df} & L_D & \\ & & kM_Q & & & L_Q \end{bmatrix} \begin{bmatrix} i_d \\ i_q \\ i_0 \\ i_f \\ i_D \\ i_Q \end{bmatrix} \quad (2.16)$$

2.1.4 Rotor angle position

The park transformation presented above depends on the rotor angle, so information of the rotor angle is required. If such a signal is not available, it has to estimate. The equation for the rotor angle is defined as eq. (2.17).

$$\gamma = \gamma(t = 0) + \frac{p}{2} \int \omega_{mech} dt - 2\pi f t \quad (2.17)$$

Where p is the number of poles of the machine, and f is the frequency. The rotor angle is defined as the angle which the d-axis leads the magnetic axis of the phase a winding, as shown in fig. 2.1. By the assumption that γ is zero after the zero-crossing of the phase a voltage, the rotor angle could be estimated by the use of a phase-locked-loop controller, a PLL, on the phase voltage measurements of phase a. A PLL is a controller that generates a signal with a phase related to the phase of the input signal.

2.2 Per unit system

In the case of a synchronous machine, the per-unit system may be used to remove arbitrary constants and simplify mathematical equations so that they may be expressed in

terms of equivalent circuits [23]. There are several ways of choosing a pu-system.

It is agreeable that using pu-units has many attractions compared to physical units, such as normalizing parameters and greatly reducing computational efforts. One difficulty with the physical units is the numerical awkwardness of the stator voltages being in the kilovolt range, while the field voltages are at a much lower level. If the per-unit system is chosen well, this can simplify greatly and even facilitate a greater understanding of system characteristics. However, as Machowski writes "Perhaps the one area in power system analysis that causes more confusion than anyother is that of per-unit systems" [1]. The many specialists in the field of have not been able to agree on one superior per-unit system, which can be used by everyone. Each pu-system has its attractions and consequently its drawbacks.

During the work on the model presented in this thesis, there had to be juggled multiple pu-systems, and Machowski as wrote, this caused a great deal of confusion. The pu model of the synchronous machine is based on the one used in [1], but the synchronous machine parameters in pu were calculated according to the equations given in [23], which use a different pu base. In this section, both pu bases are presented, but the main focus is on the one presented in [1], which form the pu model of the synchronous machine used in this thesis.

2.2.1 Stator Base Quantities

The choice for stator base quantities varies some between authors but is pretty straight forward. The almost universal choice is to choose machine ratings as the base values for the stator base quantities. Some base quantities can be chosen independently, but others follow automatically. Thus if three base quantities are chosen, which involve all three dimensions, that is voltage, current and time, all bases will be fixed for all quantities. The stator quantities are those that can be directly related to the a-b-c phase quantities through Park's transformation.

The stator base quantities used by Kundur is presented in table 2.1. Here using subscript **b** to indicate *base* and subscript **r** to indicate *rated*.

Table 2.1: Stator base quantities, Kundur

Description	Symbol	Definition	Unit
Base voltage	V_b	Peak value of line-to-neutral rated voltage	[V]
Base power	S_b	Stator rated 3-phase apparent power	[VA]
Base time	t_b	$t_b = \frac{1}{\omega_r}$	[s]
Base elec. speed	ω_b	$\omega_b = \omega_r = 2\pi f_n$	[elec. rad/sec]
Base mech. speed	ω_{mb}	$\omega_{mb} = \omega_b \frac{2}{p_f}$	[mech. rad/sec]
Base current	I_b	Peak value of rated line current, $I_b = \frac{S_b}{V_b}$	[A]
Base impedance	Z_b	$Z_b = \frac{V_b^2}{S_b}$	[Ω]
Base inductance	L_b	$L_b = \frac{Z_b}{\omega_b}$	H

This choice of stator base quantities makes the belonging inductances and reactances equal in per unit.

The stator base quantities used for the thesis model is presented in table 2.2.

Table 2.2: Stator base quantities, thesis model

Description	Symbol	Definition	Unit
Base voltage	V_b	Line to neutral RMS terminal voltage	[V]
Base power	S_b	Rated power per phase	[VA]
Base time	t_b	$t_b = 1$	[s]
Base elec. speed	ω_b	$\omega_b = \omega_r = 2\pi f_n$	[elec. rad/sec]
Base mech. speed	ω_{mb}	$\omega_{mb} = \omega_b \frac{2}{p_f}$	[mech. rad/sec]
Base current	I_b	RMS of rated line current, $I_b = \frac{S_b}{V_b}$	[A]
Base impedance	Z_b	$Z_b = \frac{V_b^2}{S_b}$	[Ω]
Base inductance	L_b	$L_b = Z_b$	H

2.2.2 Rotor base quantities

The most confusing elements of the per-unit system are introduced by the rotor base quantities. This is also where the largest differences in the two pu-systems lie. Kundur uses the rotor base quantities, which is referred to as *the L_{ad} -base reciprocal per unit system*. This pu-system has chosen the rotor base quantities to give the following advantages:

1. Per unit inductances between the different windings reciprocal, e.g, $L_{afd} = L_{fda}$.
2. Per unit mutual instances between stator and rotor circuits in each axis are equal, e.g., $L_{afd} = L_{akd}$.

In the pu system chosen by Kundur, the base current in any rotor circuit is defined as that

which induces in each phase a per unit voltage equal to per unit L_{ad} [23]. This choice of the rotor base quantities is shown in table 2.3.

Table 2.3: Rotor base quantities, Kundur

Description	Symbol	Definition	Unit
Base field current	I_{fb}	$\frac{L_{ad}}{L_{afd}} I_b$	[A]
Base damper winding current d-axis	I_{Db}	$\frac{L_{ad}}{L_{akd}} I_b$	[A]
Base damper winding current q-axis	I_{Qb}	$\frac{L_{aq}}{L_{akq}} I_b$	[A]
Base field voltage	V_{fb}	$\frac{S_b}{I_{fd}}$	[V]
Base field impedance	Z_{fb}	$Z_{fb} = \frac{V_{fb}}{I_{fb}}$	[Ω]
Base field inductance	L_{fb}	$L_{fb} = \frac{Z_{fb}}{\omega_b}$	[H]
Base damper winding impedance d-axis	Z_{Db}	$Z_{Db} = \frac{V_{fb}}{I_{Db}}$	[Ω]
Base damper winding inductance d-axis	L_{Db}	$L_{Db} = \frac{Z_{Db}}{\omega_b}$	[H]
Base damper winding impedance q-axis	Z_{Qb}	$Z_{Qb} = \frac{V_{fb}}{I_{Qb}}$	[Ω]
Base damper winding inductance q-axis	L_{Qb}	$L_{Qb} = \frac{Z_{Qb}}{\omega_b}$	[H]

The rotor base quantities used for the thesis model is chosen to be the *equal mutual flux linkages system*, that is defined by Anderson and Foud in [24], also found in [1]. This system is defined such that the mutual flux linkage in each winding is equal. By the use of this pu-system, the number of parameters is significantly reduced.

Before defining the rotor bases, it is convenient to split each individual self-inductance, L_x into its magnetizing component, L_{mx} , and leakage component, l_x . The assumption that mutual flux linkage in each winding is equal together with eq. (2.8), gives the flux linkage in each winding as defined in eq. (2.18)

$$d\text{-coil} : \quad L_{md}I_b = kM_D I_{Db} = kM_f I_{fb}$$

$$\begin{aligned}
 D\text{-coil} : \quad kM_D I_b &= L_{mD} I_{Db} = l_f I_{fb} \\
 f\text{-coil} : \quad kM_f I_b &= l_f I_{Db} = L_{mf} I_{fb} \\
 q\text{-coil} : \quad L_{mq} I_b &= kM_Q I_{Qb} \\
 Q\text{-coil} : \quad kM_Q I_b &= L_{mQ} I_{Qb}
 \end{aligned} \tag{2.18}$$

Previously it was explained how the coefficient, k , in the dq0-transformation was chosen such that to make the transformation power invariant. This comes in handy now, as the power base is same and equal for each winding: $S_b = V_b I_b = V_{fb} I_{fb} = V_{Db} I_{Db} = V_{Qb} I_{Qb}$. This fact together with eq. (2.18), produce the rotor scaling factor which can be defined as the following:

$$\frac{V_{fb}}{V_b} = \frac{I_b}{I_{fb}} = \sqrt{\frac{L_{mf}}{L_{md}}} = \frac{kM_f}{L_{md}} = \frac{L_{mf}}{kM_f} = \frac{l_f}{kM_D} \equiv k_f \tag{2.19}$$

$$\frac{V_{Db}}{V_b} = \frac{I_b}{I_{Db}} = \sqrt{\frac{L_{mD}}{L_{md}}} = \frac{kM_D}{L_{md}} = \frac{L_{mD}}{kM_D} = \frac{l_f}{kM_f} \equiv k_D \tag{2.20}$$

$$\frac{V_{Qb}}{V_b} = \frac{I_b}{I_{fQ}} = \sqrt{\frac{L_{mQ}}{L_{mq}}} = \frac{kM_Q}{L_{mq}} = \frac{L_{mQ}}{kM_Q} \equiv k_Q \tag{2.21}$$

The rotor base quantities used in this thesis can now be summed up by table 2.4.

Table 2.4: Rotor base quantities, thesis

Description	Symbol	Definition	Unit
Base field current	I_{fb}	$\frac{I_b}{k_f}$	[A]
Base field voltage	V_{fb}	$\frac{S_b}{I_{fd}}$	[V]
Base field impedance	Z_{fb}	$Z_{fb} = \frac{V_{fb}}{I_{fb}} = k_f^2 Z_b$	[Ω]
Base field inductance	L_{fb}	$L_{fb} = Z_{fb}$	[H]
Base field mutual inductance	M_{fb}	$M_{fb} = \frac{V_{fb}}{I_b} = \frac{V_b}{I_{fb}} = k_f L_b$	[H]
Base damper winding impedance d-axis	Z_{Db}	$Z_{Db} = \frac{V_{fb}}{I_{Db}} = k_D^2 Z_b$	[Ω]
Base damper winding inductance d-axis	L_{Db}	$L_{Db} = Z_{Db}$	[H]
Base damper mutual inductance d-axis	M_{Db}	$M_{Db} = \frac{V_{Db}}{I_b} = \frac{V_b}{I_{Db}} = k_D L_b$	[H]
Base damper winding impedance q-axis	Z_{Qb}	$Z_{Qb} = \frac{V_{fb}}{I_{Qb}} = k_D^2 Z_b$	[Ω]
Base damper winding inductance q-axis	L_{Qb}	$L_{Qb} = Z_{Qb}$	[H]
Base damper mutual inductance q-axis	M_{Qb}	$M_{Qb} = \frac{V_{Qb}}{I_b} = \frac{V_b}{I_{Qb}} = k_Q L_b$	[H]
Base mutual inductance f and D winding coupling	L_{fDb}	$L_{fDb} = \frac{V_{fb}}{I_{Db}} = \frac{V_{Db}}{I_{fb}} = k_f k_D L_b$	[H]

By this choice of pu system all the per-unit values of all the mutual inductance on one axis is equal:

$$L_{md} = L_{mf} = L_{mD} \equiv L_{ad}, \quad L_{mq} = L_{mQ} \equiv L_{aq} \quad (2.22)$$

After converting the system equations into per-unit values, the matrix equation of the machine from eq. (2.16) can be normalized as shown in eq. (2.23).

used is shown in fig. 2.3.

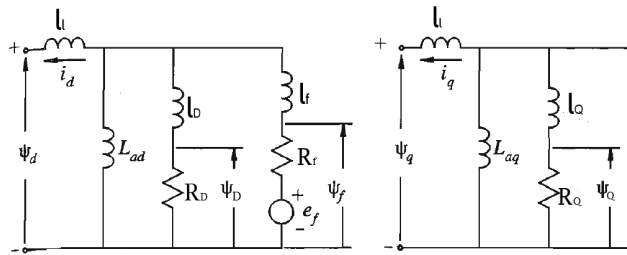


Figure 2.3: Equivalent circuit commonly used for synchronous machines

The parameters of the synchronous machine are divided into three: the subtransient, transient and sustained parameters. After a disturbance, currents are induced in the rotor, where some currents decay faster than others. The machine parameters which influence the rapidly decaying components are called the subtransient parameters, and the ones which influence the slowly decaying components are called the transient parameters. In addition, the synchronous parameters influence the sustained parameters.

The characteristics of the machine of interest are the inductances and reactances as seen from the terminals that are associated with the fundamental frequency currents during sustained, transient and subtransient conditions. In addition to these parameters, the corresponding time constants which determine the rate of decay of currents and voltages form the standard parameters used in specifying synchronous machine electrical characteristics. [23].

Expressions for the standard parameters of a synchronous machine are given in section 4.4 of Kundur's Power System Stability and Control [23] which is rewritten here. The notation used here is not the same as used in [23], but the notation used in this thesis, together with a definition, is presented in table 2.5.

Table 2.5: Notation for the synchronous machine parameters used in this thesis

Symbol	Definition
R	Stator resistance per phase
R_f	Rotor resistance
l_f	Leakage inductance field
L_f	Rotor field inductance
L_d	Stator self inductance d-axis
L_q	Stator self inductance q-axis
l_l	Leakage inductance
L_{ad}	Mutual inductance d-axis
L_{aq}	Mutual inductance q-axis
R_D	Damper winding resistance d-axis
R_Q	Damper winding resistance q-axis
l_D	Damper winding inductance d-axis
l_Q	Damper winding inductance q-axis

After converting to pu-values, it is convenient to separate the self-inductance into its magnetizing and leakage inductance. The stator self inductances, L_d and L_q , are associated with the total flux linkages due to i_d and i_q respectively and can be split into to the leakage inductance due to flux which does not link any rotor circuit and the mutual inductance due to flux that links the rotor circuits.

For the direct-axis the expressions are:

$$L_d = L_{ad} + l_l \quad (2.25)$$

$$T'_{do} = \frac{L_{ad} + l_f}{R_f} + \frac{L_{ad} + L_D}{R_D} \approx \frac{L_{ad} + l_f}{R_f} \quad (2.26)$$

$$T'_d = \frac{1}{R_f} \left(l_f + \frac{L_{ad} l_l}{L_{ad} + l_l} \right) + \frac{1}{R_D} \left(L_D + \frac{L_{ad} l_l}{L_{ad} + l_l} \right) \approx \frac{1}{R_f} \left(l_f + \frac{L_{ad} l_l}{L_{ad} + l_l} \right) \quad (2.27)$$

$$T''_{do} = \frac{1}{T_{do} R_D R_f} \left(L_D + \frac{L_{ad} l_f}{L_{ad} + l_f} \right) (L_{ad} + l_f) \approx \frac{1}{R_D} \left(L_D + \frac{L_{ad} l_f}{L_{ad} + l_f} \right) \quad (2.28)$$

$$T_d'' = \frac{1}{T_d' R_D R_f} \left(l_f + \frac{L_{ad} l_l}{L_{ad} + l_l} \right) \left(L_D + \frac{L_{ad} l_l l_f}{L_{ad} + l_l + l_f} \right) \approx \frac{1}{R_D} \left(L_D + \frac{L_{ad} l_l l_f}{L_{ad} + l_l + l_f} \right) \quad (2.29)$$

$$L_d' = L_d \frac{T_d'}{T_{d\sigma'}} \quad (2.30)$$

$$L_d'' = L_d' \frac{T_d''}{T_{d\sigma''}} \quad (2.31)$$

Similarly for the q-axis for salient pole machines:

$$L_q = L_{aq} + l_l \quad (2.32)$$

$$L_q'' = l_l + \frac{L_{aq} L_D}{L_{aq} + L_D} \quad (2.33)$$

$$T_{q\sigma}'' = \frac{L_{aq} + L_Q}{R_Q} \quad (2.34)$$

2.3 Noise filtering

When measuring currents and voltages on a machine, there is always going to be noise present. Generating stations are especially notorious for both measurement error and large amounts of noise due to high currents and voltages [25]. Therefore, when dealing with synchronous machine measurements, there is always a need for some sort of noise filtering. There are various types of noise which require different filtering. Noise is often divided into white and non-white noise. Where white noise is characterized as a sequence of independent, equally distributed, Gaussian, random variables of zero mean value and variance σ^2 [26]. With white noise, there is no correlation between the noise and the signal. Generally, however, a disturbance in a signal or measurement is not just white noise. With non-white noise, there could be a clear correlation between the noise and the signal, making it harder to filter.

Many different filters have been developed for the purpose of noise filtering. The filters used for this purpose are the digital discrete filters, where some essential mentions are

the moving-average filters, Butterworth, Chebyshev and Bessel.

One disadvantage of using a filter is that it always introduces a phase shift or delay to the filtered signal. However, when the synchronous machine is only analyzed during steady-state, this is not so crucial, but the fact is important to remember if the one were to study the synchronous machine under transient conditions. If transient conditions were to be studied, it would be desirable to implement a zero-phase digital filter.

2.3.1 Kalman Filter

After discussing noise and how this appears together with the signals in measurements from the machine, there is a need to discuss solutions for this. A solution for the separating random noise signal itself is by the use of a Kalman Filter. The Kalman Filter was introduced by Rudolf E. Kálmán in 1960, and he solves the problem of separating signal from random noise with a "state" point of view [27]. This was done by defining the noisy measurements to be a discrete sequence instead of a continuous signal. In the model of estimation the parameters of the synchronous machine used in for this thesis, the Kalman filter is used as an optimal observer with the primary goal of filtering and correcting measurements by using prior knowledge about the synchronous machine and its parameters. The following theory presented about the Kalman filter is based on the theory from [28].

The Kalman filter revolutionized the field of estimation, as it can be used to both reconstruct unmeasured states in addition to removing white and coloured noise from state estimates. The main approach of the Kalman is to improve the prior estimate by using measurements. Kalman filtering is used in this thesis model for both as an observer for the damper winding currents, as there are no measurements for these, in addition to removing noise from measurements.

Consider a basic dynamic system presented as a state-space model:

$$\mathbf{x}_{k+1} = \mathbf{A}_k \mathbf{x}_k + \mathbf{B}_k (\mathbf{u}_k + \mathbf{w}_k)$$

$$\mathbf{y}_k = \mathbf{C}_k \mathbf{x}_k + \mathbf{v}_k$$

The state-space model is given on its discrete form and is the result of sampling a continuous-time measurements. Here \mathbf{x}_k is the process state vector at time t_k . The matrices \mathbf{A} and \mathbf{B} are known and \mathbf{w} is the assumed white noise of the input signal, \mathbf{u} . \mathbf{y}_k is defined as the vector measurement at time t_k and \mathbf{v} is measurement error for \mathbf{y}_k , and is assumed to be white and having zero cross-correlation with the input noise sequence.

The covariance matrices of the noise are assumed known and characterized by:

$$E[\mathbf{w}_k \mathbf{w}_i^T] = \begin{cases} \mathbf{Q}_k, & i = k \\ \mathbf{0}, & i \neq k \end{cases}$$

$$E[\mathbf{v}_k \mathbf{v}_i^T] = \begin{cases} \mathbf{R}_k, & i = k \\ \mathbf{0}, & i \neq k \end{cases}$$

$$E[\mathbf{w}_k \mathbf{v}_i^T] = \mathbf{0} \text{ for all } k \text{ and } i$$

The process of the Kalman filter can be visualized with fig. 2.4.

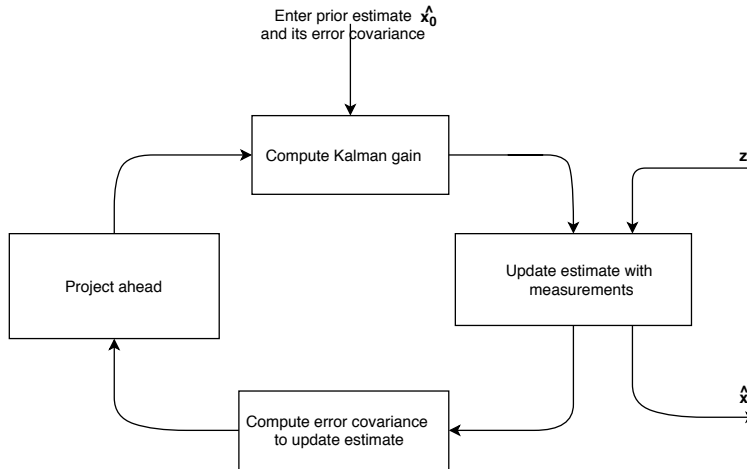


Figure 2.4: The Kalman filter loop.

First, a *a priori* estimate, $\hat{\mathbf{x}}_k$, is defined, which is an initial estimate of the process at a given time t_k and is based on all the knowledge prior to this time. The estimation for this *a priori* estimate is defined as $\mathbf{e}_k^- = \mathbf{x}_k - \hat{\mathbf{x}}_k$, with a covariance matrix is \mathbf{P}_k^- . The next step is to now update and improve the estimation by using the measurement, \mathbf{y}_k and the blending factor, \mathbf{K}_k . The blending factor, \mathbf{K}_k , is computed in order to minimize the estimation error and tells the system how much it should rely on measurements contra the estimate from the Kalman filter.

The updated (a posteriori) estimate will then be:

$$\hat{\mathbf{x}}_k = \hat{\mathbf{x}}_k + \mathbf{K}_k (\mathbf{y}_k - \mathbf{C}_k \hat{\mathbf{x}}_k^-)$$

After this, the a posteriori estimate will be used to re-compute the error covariance and used in the next step to project ahead and predict a new \mathbf{x}_k^- . The algorithm will continue to repeat itself in the Kalman filter loop that is illustrated in fig. 2.4.

The Kalman Filter presented above is the discrete Kalman Filter, which is the original Kalman Filter and is the one used for the model in this thesis. However, the Kalman filter also has a continuous counterpart, as well as an unscented and extended version which can be used for nonlinear systems.

2.4 Recursive Least Squares algorithm

In addition to noise filtering and state observing, an algorithm for the actual parameter estimation has to be chosen. Parameter estimation can be defined as the process of giving a value to a system variable, where the actual value is unknown, based on some criteria. There are many different methods and algorithms for performing parameter estimation, such as infinite -norm, and 1-norm, or least-squares estimators. In this thesis, the algorithm chosen is the Recursive Least Squares algorithm due to its fitness and availability in the System Identification Toolbox of Simulink. The RLS algorithm is good for real-time settings, where the 'true' underlying parameters are changing over time [29]. The RLS algorithm is not so dissimilar to the Kalman Filter, and the former can be considered a special case of the latter [30]. With perfect knowledge of how the actual system varies, the Kalman filter provides a natural framework for the estimation [31].

It is well-known that a constant value of this parameter leads to a compromise between misadjustment and tracking. When the value of the forgetting factor is very close to 1, the algorithm achieves good misadjustment but poor tracking. [32]

2.4.1 Recursive Least Squares Parameter Equations

Recursive least squares (RLS) is a statistical framework involving a probabilistic treatment of observational errors and was developed by Karl Frederick Gauss in 1809 [33]. In the context of adaptive filtering, the recursive least-squares (RLS) is a very popular algorithm, especially for its fast convergence rate. Firstly, let's define an estimate of an arbitrary parameter as, $\hat{\theta}_t$, where the 'hat' denotes it as an estimation and the subscript, t , denotes the iteration number. Online recursive identification methods compute the parameter estimations recursively over time. At iteration t , new observations have become available and these are used to modify a the estimate, $\hat{\theta}_{t-1}$ which was computed at iteration $t - 1$.

Given a linear regression signal model on the form:

$$y_t = \varphi_t^T \theta + e_t, \quad \forall t = 1, 2, \dots \quad (2.35)$$

where y_t and φ_t are known signals, θ is the unknown parameters which are to be estimated and e_t is zero mean value noise of some form.

The most popular approach to deal with time-varying linear regression is to minimize a cost function:

$$V_t(\theta) = \sum_{k=1}^t \beta(t, k) (y_k - \theta^T \varphi_k)^2$$

where

$$\beta(t, k) = \prod_{j=k+1}^t \lambda_j$$

and where $0 \leq \lambda \leq 1$ is called the forgetting factor. If λ is set to a value smaller than one, less weight will be given to older observation. The smaller λ gets, the quicker older observations will be forgotten. The use of the forgetting factor is such that the RLS algorithm can track time-varying parameters, where the true parameter vector varies over time. It is well-known that a constant value of the forgetting-factor leads to a compromise between misadjustment and tracking. When the value of the forgetting factor is very close to 1, the algorithm achieves good misadjustment but poor tracking. [32] The algorithm aims to minimize the error between the observed and predicted outputs.

The general algorithm for recursive least squares that minimizes the cost function is written as follows in eq. (2.36).

$$\hat{\theta}_t = \hat{\theta}_{t-1} + L_t \epsilon_t \quad (2.36a)$$

Where the error of the approximation, ϵ is given by

$$\epsilon_t = y_t - \varphi_t^T \hat{\theta}_{t-1} \quad (2.36b)$$

The gain vector L_t is given by

$$L_t = \frac{P_{t-1} \varphi}{\hat{R}_{2t} \varphi^T(t) P_{t-1} \varphi} \quad (2.36c)$$

and the matrix $P(t)$ is updated by

$$P_t = P_{t-1} - \frac{P_{t-1}\varphi_t\varphi_t^T P_{t-1}}{\hat{R}_{2t} + \varphi_t^T P_{t-1}\varphi(t)} + \hat{R}_1 \quad (2.36d)$$

Where \hat{R}_1 and \hat{R}_2 are the covariance matrices of the white Gaussian noise to θ_0 and y , respectively. The term ϵ_t is interpreted as the prediction error, and is the difference between observed sample, and the predicted value. If this value is small, the estimation is good, and does not need to be modified much. The important issue on choosing the initial values, P_0 and $\hat{\theta}_0$, for the RLS algorithm will be revisited later in the thesis. Throughout the rest of the thesis, the following notation will be used:

Table 2.6: Notation for RLS parameters used in thesis

θ		The 'true' value for a given parameter
$\hat{\theta}_t$		The estimation of the given parameter
θ_0		The 'true' initial condition of a given parameter
$\hat{\theta}_0$		The estimation of the initial condition of a given parameter

Chapter 3

Method and model

3.1 Creation of a State-Space Representation

The synchronous machine model is assumed to be a linear time-invariant system, meaning its parameters are constant and independent of time. The state-space-equations are to be written on the form shown in eq. (3.1).

$$\dot{\mathbf{x}}(t) = \mathbf{A}\mathbf{x}(t) + \mathbf{B}\mathbf{u}(t) \quad (3.1a)$$

$$\mathbf{y}(t) = \mathbf{C}\mathbf{x}(t) + \mathbf{D}\mathbf{u}(t) \quad (3.1b)$$

Where the vectors, \mathbf{x} , \mathbf{y} , and \mathbf{u} , are the states, outputs, and inputs, respectively.

By looking at eq. (2.23) it would be natural to assume $\mathbf{y} = \mathbf{x} = [i_d, i_q, i_0, i_f, i_D, i_Q]^T$ and $\mathbf{u} = [v_d, v_q, v_0, v_f, v_D, v_Q]^T$ and thereby $\mathbf{A} = -\mathbf{L}_{sm}^{-1}\mathbf{R}_{sm}$, $\mathbf{B} = \mathbf{L}_{sm}^{-1}$, $\mathbf{C} = \mathbf{I}$ and $\mathbf{D} = \mathbf{0}$.

However for control purposes, the input vector is chosen to be $\mathbf{u} = [i_d, i_q, i_0, v_f, v_D, v_Q]^T$, as these are all affected by external factors. The currents are defined by the load of the machine, v_f is given by the excitation system and v_D and v_Q are zero as the damper windings are short-circuited. The output vector will then be defined as $\mathbf{y} = [v_d, v_q, v_0, i_f, i_D, i_Q]^T$.

Before completing the state-space, it is helpful to define a star-connected dummy load of $R_{dl}=10^4$ pu that is connected to the voltage terminals. As R_{dl} is so large, the voltage

drop across the resistance can be neglected.

The stator voltages in the rotor reference frame can then be expressed as:

$$v_d = R_{dl}(i_d - i_{dt}) \quad v_q = R_{dl}(i_q - i_{qt}) \quad v_0 = R_{dl}(i_0 - i_{0t})$$

Equation (2.23) can then be written as eq. (3.2) and the state space can be expressed as eq. (3.3), as obtained in [6].

$$\begin{aligned}
 \begin{bmatrix} R_{dl}i_{dt} \\ R_{dl}i_{qt} \\ R_{dl}i_{0t} \\ v_f \\ 0 \\ 0 \end{bmatrix} &= \overbrace{\begin{bmatrix} R + R_{dl} & \omega(L_{aq} + l_l) & & & & \omega L_{aq} \\ -\omega(L_{aq} + l_l) & R + R_{dl} & & & & \\ & & R + 3R_N + R_{dl} & & & \\ & & & R_f & & \\ & & & & R_D & \\ & & & & & R_Q \end{bmatrix}}^{\mathbf{R}_{sm,dl}} \begin{bmatrix} i_d \\ i_q \\ i_0 \\ i_f \\ i_D \\ i_Q \end{bmatrix} \\
 -\frac{d}{dt} \begin{bmatrix} L_{ad} + l_l & & & & & & \\ & L_{aq} + l_l & & & & & \\ & & L_0 + 3L_N & & & & \\ & & & L_{ad} & L_{ad} & & \\ & L_{ad} & & L_{ad} + l_f & L_{ad} & & \\ & L_{ad} & & L_{ad} & L_{ad} + l_D & & \\ & & L_{aq} & & & L_{aq} + l_Q & \end{bmatrix} \begin{bmatrix} i_d \\ i_q \\ i_0 \\ i_f \\ i_D \\ i_Q \end{bmatrix} \\
 &\underbrace{\hspace{15em}}_{\mathbf{L}_{sm}} \tag{3.2}
 \end{aligned}$$

$$\mathbf{u} = [R_{dl}i_{dt} \quad R_{dl}i_{qt} \quad R_{dl}i_{d0} \quad v_f \quad 0 \quad 0]^T$$

$$\mathbf{y} = [v_d \quad v_q \quad v_0 \quad i_f \quad i_D \quad i_Q]^T \quad \mathbf{x} = [i_d \quad i_q \quad i_0 \quad i_f \quad i_D \quad i_Q]^T$$

$$\mathbf{A} = -\mathbf{L}_{sm}^{-1} \mathbf{R}_{sm,dl} \quad \mathbf{B} = \mathbf{L}_{sm}^{-1} \tag{3.3}$$

$$\mathbf{C} = \begin{bmatrix} R_{dl} & & & & & \\ & R_{dl} & & & & \\ & & R_{dl} & & & \\ & & & 1 & & \\ & & & & 1 & \\ & & & & & 1 \end{bmatrix} \quad \mathbf{D} = \begin{bmatrix} -1 & & & & & \\ & -1 & & & & \\ & & -1 & & & \\ & & & -1 & & \\ & & & & 0 & \\ & & & & & 0 \\ & & & & & & 0 \end{bmatrix}$$

3.2 Observer for damper winding currents

One obvious problem with the state-space representation in eq. (3.3), is that there are often no available measurements for the damper winding currents i_D and i_Q , but these appear in both \mathbf{x} and \mathbf{y} . This problem can be solved in two ways, either if only steady-state analysis is to be performed, the damper currents can be assumed to be zero, or a state observer can be created, as done in [10], [34] and [25]. For this model, the latter is chosen so that the damper winding resistances also can be estimated. By examining eq. (3.2), it is possible to use the last two rows of the matrix equation to create expressions for the currents. The state observer generates an estimation of the unknown damper winding currents as an output. The initial values of i_D and i_Q are assumed to be zero without loss of accuracy, which can be proved by the final value theorem.

The expression for the damper windings by rearranging the last two lines of eq. (3.2) can be written as shown in eq. (3.4).

$$i_D = -\frac{sL_{ad}}{s(L_{ad}) + R_D}(i_d + i_f) \quad i_Q = -\frac{sL_{aq}}{s(L_{aq}) + R_Q}i_q \quad (3.4)$$

3.3 Calculate Parameters of the Synchronous Generator

The parameter estimation algorithm is created to be performed on a synchronous generator and in the case of this thesis, a salient pole synchronous generator with five pole pairs from Voith situated in a German Hydro plant. The data received about the synchronous generator from the manufacture is a datasheet including the rated data, and the standard parameters of the machine collected from short- and open-circuit tests. From this rated data and standard parameters, the electrical parameters that are needed to complete the state-space representation of the machine, on the form of eq. (3.3), can be calculated.

In addition to the standard parameters, one parameter is wanted, namely the stator leakage inductance, to avoid an iterative process when calculating the electrical parameters.

This parameter represents the amount of leakage flux in the stator of the machine, and together with the armature inductance, the leakage inductance forms the self-inductances, L_d and L_q . The leakage inductance value is not traditionally included in the datasheets of synchronous generators, but for a salient-pole synchronous generator, the typical value of the stator leakage inductance is between 0.1 - 0.2 p.u [23]. By knowing this, the leakage inductance can be initially guesstimated and updated after the parameter estimation. However, for the machine modelled in this thesis, the leakage inductance is fortunately known, so the iterative process is avoided.

By the use of the equations eq. (2.25) - (2.34) presented presented in section 2.2.3, it is possible to calculate the corresponding electrical parameters which are included in the state space equations of the machine and needed for the parameter estimation, which are L_{ad} , L_{aq} , R_f , l_f , l_Q , R_D , R_Q , l_Q .

Initially the electrical parameters were attempted to be calculated from equations (2.25) - (2.34) by using the Matlab function `solve`. However, due to small discrepancies and errors in the standard parameters, there was no solution which made all the equations to be fulfilled perfectly. Therefore, to be able to calculate the parameters there had to be done some approximations by making some reasonable assumptions.

The standard parameters can also be expressed with expressions from inspection of the equivalent circuit. This is done by the introduction of the series inductance L_{pl} , which corresponds to the peripheral flux that links the field and the damper and is given by eq. (3.5).

$$L_{pl} = L_{fD} - L_{ad} \quad (3.5)$$

By the assumption that the rotor resistance, R_f , is zero during subtransient periods and that the damper resistance, R_D , is infinitely large during transient periods. After defining L_{pl} , it is also common to assume $L_{fkD} = L_{ad}$, such that $L_{pl} = 0$ [23]. This assumption is reasonable as the flux linking the damper circuit is almost equal to that linking the armature, as the damper windings are near the air-gap. The approximate expressions for the standard parameters for the d-axis can then be written as follows:

$$L_d = L_{ad} + l_l \quad (3.6)$$

$$L'_d = l_l + \frac{1}{\frac{1}{L_{ad}} + \frac{1}{l_f}} \quad (3.7)$$

$$L''_d = l_l + \frac{l_D l_f L_{ad}}{L_{ad} l_f + L_{ad} l_D + l_D l_f} \quad (3.8)$$

$$T'_{do} = \frac{L_{ad} + l_f}{R_f} \quad (3.9)$$

$$T''_{do} = \frac{1}{R_D} \left(l_D + \frac{l_f L_{ad}}{l_f + L_{ad}} \right) \quad (3.10)$$

$$T'_d = \frac{1}{R_f} \left(l_f + \frac{L_{ad} l_l}{L_{ad} + l_l} \right) \quad (3.11)$$

$$T''_d = \frac{1}{R_D} \left(l_D + \frac{L_{ad} l_l l_f}{l_f L_{ad} + l_f l_l + L_{ad} l_l} \right) \quad (3.12)$$

For laminated salient-pole machines, such as the one modelled in this thesis, the only circuit in the rotor for the q-axis is the damper winding. The expressions for the q-axis parameters are equal to the ones presented in section 2.2.3 and are repeated here:

$$L_q = l_l + L_{aq} \quad (3.13)$$

$$L''_q = l_l + \frac{L_{aq} l_Q}{L_{aq} + l_Q} \quad (3.14)$$

$$T''_{q0} = \frac{L_{aq} + l_Q}{R_Q} \quad (3.15)$$

As Kundur [23] shows that the deviation between the accurate and approximate values of the parameters are insignificant for the parameters, the approximate equations presented above could be used to calculate the parameters.

Firstly the mutual inductances, L_{ad} and L_{aq} , were calculated by the use of eq. (3.6) and eq. (3.13), respectively. Secondly the leakage inductance of the field winding, l_f , could also be computed by the means of eq. (3.7). R_f could then be computed from eq. (3.9). Lastly, the damper inductances and resistances of the d- and q-axis, l_D , l_Q , R_D and R_Q , are calculated by eq. (3.8), eq. (3.14), eq. (3.10) and eq. (3.15), respectively. The only equations not used to calculate a parameter is then eq. (3.11) and eq. (3.12), but since all parameters included are known, they could be used to validate values.

One important thing to notice is that the equations above of the standard parameters are valid when using the pu-system introduced by Kundur in [23], but not for all pu-systems. Before the pu values from the equations above can be used in the model, they have to be converted between the two pu-systems presented in section 2.2.

3.4 Simulink Model

After the parameters and pu-bases are calculated, the model of the machine can be implemented in Simulink. The model built in Simulink is based on the model which Erick Alves created for his master thesis, [6]. A brief explanation of the model implemented in MATLAB and Simulink is presented in this section.

3.4.1 Testing Parameter Estimation using real data

A goal of this master thesis was to validate the parameter estimation algorithm with the use of actual data from a generator, not only data produced by a Synchronous Machine block from Simulink as done in [6] and [5]. The goal of the algorithm is to correctly estimate the standard parameters of the machine given in the datasheet. If this is successful, the algorithm could possibly be used to track generator parameters over time to potentially prevent system outages, without ever having to take the machine of the grid.

From Voith, 300 seconds data of phase currents, voltages and in addition, the field current and voltage during the steady-state operation was received. This data was collected and measured without taking the generator off the grid while the generator was running at rated load. The data had a high-frequency sampling of 2000 Hz.

In addition to the voltages and currents from the generator, information about the rotor angle, δ , is needed before the parameter estimation can be performed. There are several ways the rotor angle position can be estimated, some far more complicated than others. For this thesis, simplicity was preferred, and a PLL was chosen to estimate the rotor angle. This choice was made as the PLL is already readily available in the System Identification Toolbox of Simulink.

The measurements of the phase voltages and currents, v_{abc} , and i_{abc} , and field voltage and current, v_f and i_f , are uploaded to Matlab and sent to Simulink using a "from workspace" block. There were used 30 seconds of measurements starting when the phase a stator voltage had its zero crossings when the rotor angle is assumed to be zero. The measurements replace the synchronous machine block from Matlab in the original model.

When using actual measurements, there is now neither necessary nor wanted to add extra noise or re-sampling. The Simulink model using the measurements from the Voith generator is shown in fig. 3.1.

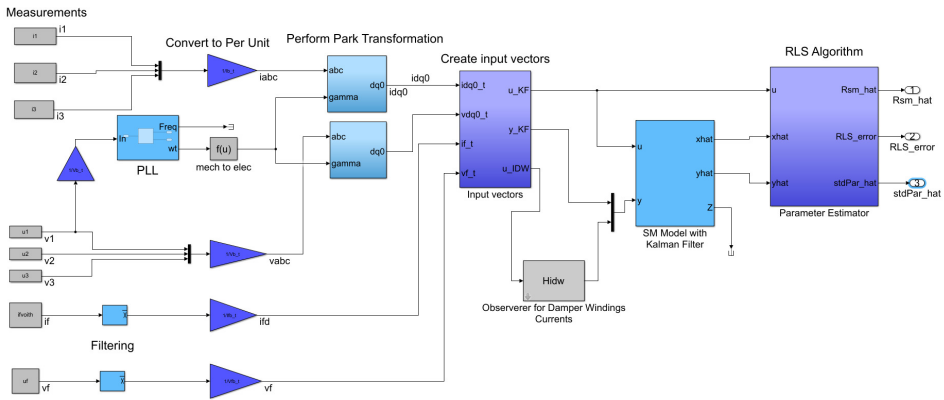


Figure 3.1: Simulink model using real measurements from a synchronous generator

The measurements are then converted to their per-unit values, using the bases stated in table 2.2 and table 2.4. The "PLL"-block takes in the phase a voltage in pu as input and returns the rotor angle position. The PLL was tuned some, but it was not used an excessive time doing this. The rotor position is then converted from mechanical into electrical units by eq. (2.1).

The stator phase voltages and currents can now be transformed into the rotor reference frame using the park transformation explained in section 2.1.2. After this the \mathbf{u} , \mathbf{y} vector are created as presented in eq. (3.3). The damper winding currents are then estimated by use of the observer created eq. (3.4). The vector of \mathbf{u} and \mathbf{y} can then be fed to the Kalman filter together with the discretised transfer function of the \mathbf{A} , \mathbf{B} , \mathbf{C} , and \mathbf{D} matrices from eq. (3.3). An additional input to the Kalman filter is the noise covariances \mathbf{Q} and \mathbf{R} . The elements of \mathbf{Q} and \mathbf{R} were tuned some in [6] and [5] and the matrices is presented in eq. (3.16).

$$\mathbf{Q} = \begin{bmatrix} 0.05 & & & & & \\ & 0.05 & & & & \\ & & 0.05 & & & \\ & & & 0.05 & & \\ & & & & 0.03 & \\ & & & & & 0.03 \end{bmatrix} \quad \mathbf{R} = \begin{bmatrix} 0.05 & & & & & \\ & 0.05 & & & & \\ & & 0.05 & & & \\ & & & 0.05 & & \\ & & & & 0.05 & \\ & & & & & 0.05 \end{bmatrix} \quad (3.16)$$

The values for \mathbf{Q} and \mathbf{R} were proven to produce robust results in several load conditions and values of noise [6]. The Kalman filter is used for state estimation and has $\hat{\mathbf{x}}$ and $\hat{\mathbf{y}}$ as outputs. $\hat{\mathbf{x}}$ and $\hat{\mathbf{y}}$, are then together with \mathbf{u} sent to the RLS algorithm to perform the parameter estimation. The RLS-estimator estimates the parameters of R_{sm} -matrix by assuming steady-state of the machine. During steady-state $\frac{d}{dt}\mathbf{i}_{dq0fDQ} = 0$, and the equation of the voltages, eq. (2.23), can be written as shown in eq. (3.17).

$$\begin{bmatrix} v_d \\ v_q \\ v_0 \\ v_f \\ 0 \\ 0 \end{bmatrix} = - \begin{bmatrix} R & \omega(L_{aq} + l_l) & & & & \\ -\omega(L_{aq} + l_l) & R & & & & \\ & & R + 3R_N & & & \\ & & & R_f & & \\ & & & & R_D & \\ & & & & & R_Q \end{bmatrix} \begin{bmatrix} i_d \\ i_q \\ i_0 \\ i_f \\ i_D \\ i_Q \end{bmatrix} \quad (3.17)$$

or in its compact format:

$$\mathbf{v}_{dq0fDQ} = -\mathbf{R}_{sm}\mathbf{i}_{dq0fDQ} \quad (3.18)$$

The RLS-estimator use Recursive least squares estimation, as explained in section 2.4.1. The RLS estimator uses the measurements/estimates of \mathbf{v}_{dq0fDQ} and \mathbf{i}_{dq0fDQ} to provide an estimate for \mathbf{R}_{sm} . Each element in \mathbf{R}_{sm} is then estimated by its own RLS-estimator block using the corresponding currents and voltages according to eq. (3.17). The RLS-estimator block has P_0 , λ and $\hat{\theta}_0$ as inputs, where P_0 is chosen as 0.05, $\lambda = 0.998$ (corresponding to a memory horizon of 10 seconds), and $\hat{\theta}_0$ is set according to the calculated pu values found stated in table 4.1 and table 4.3. The latter means that $\hat{\theta}_0$ is chosen equal to θ , the true value. The block uses the initial parameter estimate at the beginning of a

simulation or when the algorithm is triggered by using the reset signal [35].

When steady-state is assumed, it is not possible to estimate \mathbf{L}_{sm} ; however, 4 out of 8 parameters from \mathbf{L}_{sm} are also represented in \mathbf{R}_{sm} . But when \mathbf{L}_{sm} is not estimated, not all parameters which are included in eq. (2.25) - (2.34) is estimated, thereby not possible to create complete estimates of the standard parameters. In addition, the stator phase resistance, \mathbf{R} , from \mathbf{R}_{sm} is not estimated as it is much smaller than the other parameters and therefore hard to estimate.

To ensure that the parameter estimation is only performed during steady-state, the RLS-estimator-block is only enabled when i_D and i_Q is below a threshold value of 0.005 pu, which is the value where steady-state is assumed in [6]. If the damper winding currents are increased above this level, the RLS-estimator is disabled, and the estimation does not take place. Another important thing to note with this is that when the RLS-estimator is enabled after being disabled, it is reset to its initial conditions.

Results

4.1 Specifications of Machine

The synchronous generator which the parameter estimation algorithm is to be performed on is a salient pole synchronous generator from Voith in a German hydropower plant. The generator has five pole pairs, and the specifications of the generator are given below in table 4.1. The standard parameters were given in the datasheet of the machine and are re-given in table 4.2. The calculated electrical parameters which are included in the state-space representation of the machine is pretended in table 4.3.

Table 4.1: Machine rated data of the Voith salient-pole synchronous generator

Description	Symbol	Value
Voltage (line-line)	U	21 kV
Apparent effect	S	300 MVA
Power factor	ϕ	0.75
Frequency	f	50 Hz
Number of poles	p	10
Number of phases	m	3
No-load field current	I_{fn}	726 A
Stator resistance (per-phase)	R_s	5.49 m Ω
Field resistance	R_f	128.65 m Ω

Table 4.2: Standard Parameters for the Voith synchronous generator from datasheet

Reactances	Value [p.u]
X_d	1.39
X'_d	0.46
X''_d	0.44
X_q	0.98
X'_q	0.46
X''_q	0.77
Time constants	Value [s]
T'_{do}	18.38
T'_d	6.03
T''_d	0.81
T''_{do}	1.14
T''_q	0.11
T''_{qo}	0.42
Additional parameters	Value [p.u]
X_l	0.134

Table 4.2 shows the transient and subtransient reactances of the d- and q-axis in addition to the four principal d-axis time constants and the two q-axis time constants. The standard parameters presented in table 4.2 are collected from short-circuit- and open-circuit tests performed on the machine by the manufacturer. The standard parameter reactance values are given in their per-unit value with the stator base value equal to the corresponding machine rated values. The time constants are given in seconds.

From the rated data in table 4.1 and the standard parameters in table 4.2, the electrical parameters that are needed to complete the state-space representation of the machine, on the form of eq. (3.3), can be calculated. The electrical parameters of the machine are then calculated by the use of eq. (3.6) - (3.15) and the per-unit values for these are presented in table 4.3

Table 4.3: Calculated Parameters

Parameter	Description	Value [p.u]
Direct axis		
L_{ad}	Mutual inductance d-axis	1.256
L_{fd}	Leakage inductance field	0.4403
R_{fd}	Field resistance	0.3566e-3
L_f	Field inductance	1.6963
L_{1d}	Damper winding inductance	4.9878
R_{1d}	Damper winding resistance	0.0148
Quadrature axis		
L_{aq}	Mutual inductance	0.846
L_{1q}	Damper winding inductance	2.4073
R_{1q}	Damper winding resistance	0.0243

After the electrical parameters are calculated, the state-space model of the synchronous generator that is used for the parameter estimation can be created using the equations in (3.3).

4.2 Parameter Estimation with Real Measurements

The measurement data which was received for the synchronous machine from Voith was 300 seconds of phase currents and voltages and field current and voltage during steady-state of the machine running with rated load. The measurements had a frequency sampling of 2 kHz,

The rotor position of the machine information was unavailable, so this was estimated using a phase-locked-loop on the per-unit value of the phase a voltage measurements. The parameter estimation algorithm was performed with a Recursive Least Squares algorithm using Matlab and Simulink with the setup as presented in fig. 3.1. The parameters which are estimated are the ones which are included in the \mathbf{R}_{sm} , thus $R + 3R_N$, R_f , L_{ad} , L_{aq} , R_D , R_Q , X_d , and X_q . The initial parameter estimation value of the RLS-block, $\hat{\theta}_0$ is chosen to be equal to the 'true' value, θ , according to the calculated parameter values given in table 4.3. The standard parameters are not directly estimated, but can be calculated from the estimated parameters, in addition to values from table 4.3 for the parameters where the estimation is not available.

One significant problem presented itself after the generator model was created and when the parameter estimation was to be performed; the measurements of the field voltages and currents were subject to a large amount of noise which was not white. A sample of

0.5 seconds of the field voltage is shown in fig. 4.1. This noise was present in all 400 seconds of the data.

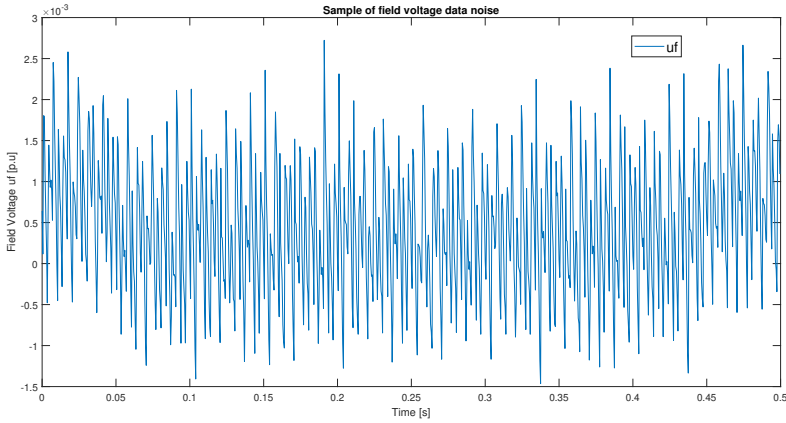


Figure 4.1: Sample of the field voltage of the Voith generator during rated load in per unit showing the noise of the signal

Figure 4.1 shows the amount of noise present at the measurements of the field voltage. It can be observed that the field voltage has a slowly varying component of about 1.25 Hz. An oscillating component of about 333.33 Hz is also present in the measurements. The same amount of noise was also present at the field current. These components are undesired as in the measurements for field current and voltage, the components of interest are at or near DC.

[6] shows that the performance of both the algorithm and the Kalman Filter was good even with high amounts of noise present, with a noise density of $10^{-9} \frac{W}{Hz}$. However, the noise which was added in [6] was band-limited white noise, and it was added to all measurements. However, the problems with the amounts of noise present in the field voltage and current in this scenario, was that the noise was not white. It, therefore, presented a problem of trying to filter out this noise as the Kalman Filter is not able to filter out non-white noise.

It would at this point have been beneficial if the measurements could be replaced with measurements with lower levels of noise, but due to the corona situation, this was not possible. There was made countless attempts of filtering the measurements with both variations of a low-pass filter, moving-average filter, and manually trying to filter out the noise based on its frequency by using the mean-block from the Simulink libraries. None of these attempts resulted in a satisfactory quality, but manually trying to find the noise

frequency and then filtering out these with high-frequency components of the signal by using "mean"-block in Matlab appeared to give a not good, but yet best result.

A problem with noisy field current measurements was that this also resulted in noisy observations of the damper winding currents. All the measurements from the generator were collected during steady-state of the machine with a rated load. During steady-state, both damper winding currents are zero in the dq0-equivalent model. However, due to the high noise present in the field current, this caused the observer for the damper winding current on the d-axis to observe a highly oscillating current for the damper windings. The plot of the d-axis damper winding current is shown in fig. 4.2.

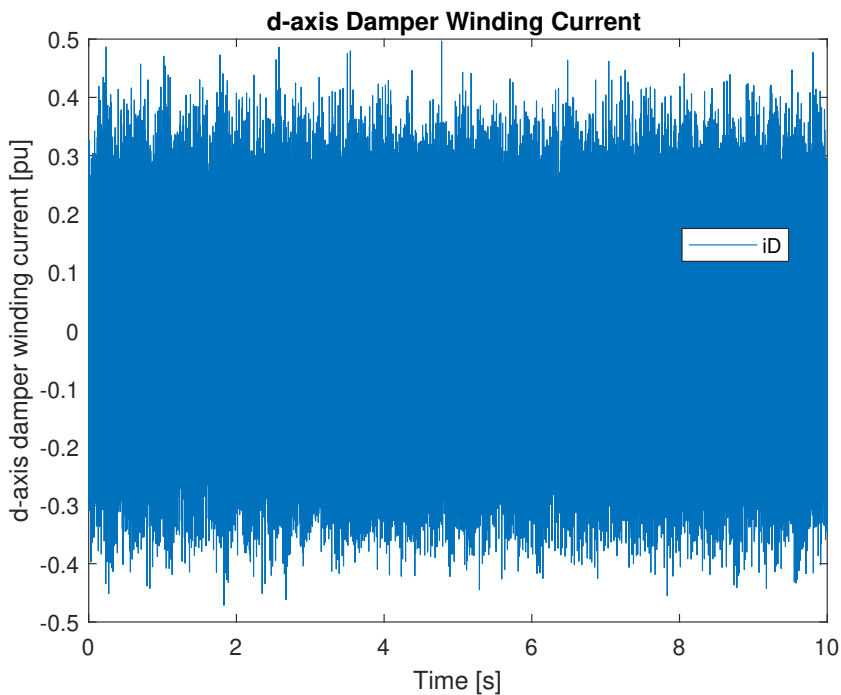


Figure 4.2: Sample of the observed d-axis damper winding current of the Voith generator during rated load. Showing the signal is clearly affected by noise.

Figure 4.2 shows that the d-axis damper winding current is affected by large amounts of noise and is oscillating with a high frequency with values from -0.5 to 0.5 pu. The oscillations in the d-axis damper winding current are due to it being a function of the field current as can be seen by eq. (3.4). A problem associated with this was that the machine is assumed to be in steady-state with values of the damper windings currents between -0.005 pu and 0.005 pu. If the values are outside of this range, the RLS-algorithm is dis-

abled and reset to its initial conditions. The RLS-block then remains disabled until the currents again were below ± 0.005 pu.

The noise in the damper winding current therefore created the problem that the oscillating value kept disabling and enabling the RLS algorithm frequently giving a highly oscillating value for $\hat{\theta}$. This problem is illustrated with the results of the parameter estimation from the RLS algorithm, shown in fig. 4.3.

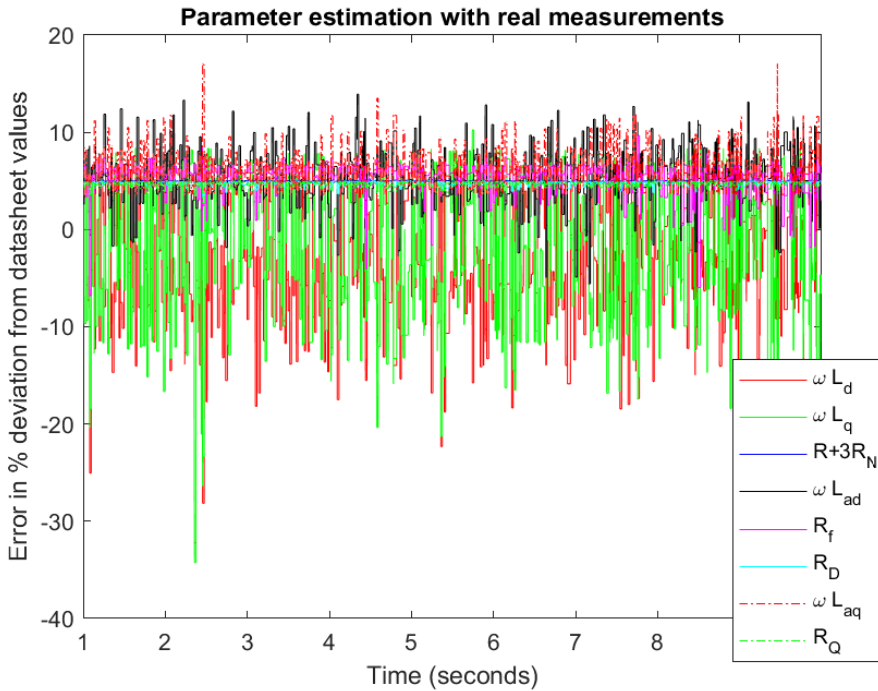


Figure 4.3: First ten seconds of the parameter estimation from the RLS-block by using noisy measurements from a real generator at rated load.

Figure 4.3 shows how the parameter estimates, $\hat{\theta}$, from RLS parameter are affected by large amounts of oscillation during the simulation. This is due to the RLS-algorithm being reset, thereby making the value of $\hat{\theta}$ again equal to the 'true' value of θ_0 .

The conclusion from the parameter estimation was that the quality of the field current and voltage was so low, that it was hard to test the algorithm and evaluate the performance of the parameter estimation. The fig. 4.3 shows that the estimation for the parameters from the RLS algorithm was highly oscillating for all parameters and it did not appear to be converging to the real value even with longer simulation time.

4.2.1 Parameter Estimation with Damper Winding Currents Set to Zero

To avoid the problem of the oscillating damper winding current shown in fig. 4.2, the same simulation was performed as explained above, only with the damper winding currents set to zero. The results from the parameter estimation for this is shown in fig. 4.4.

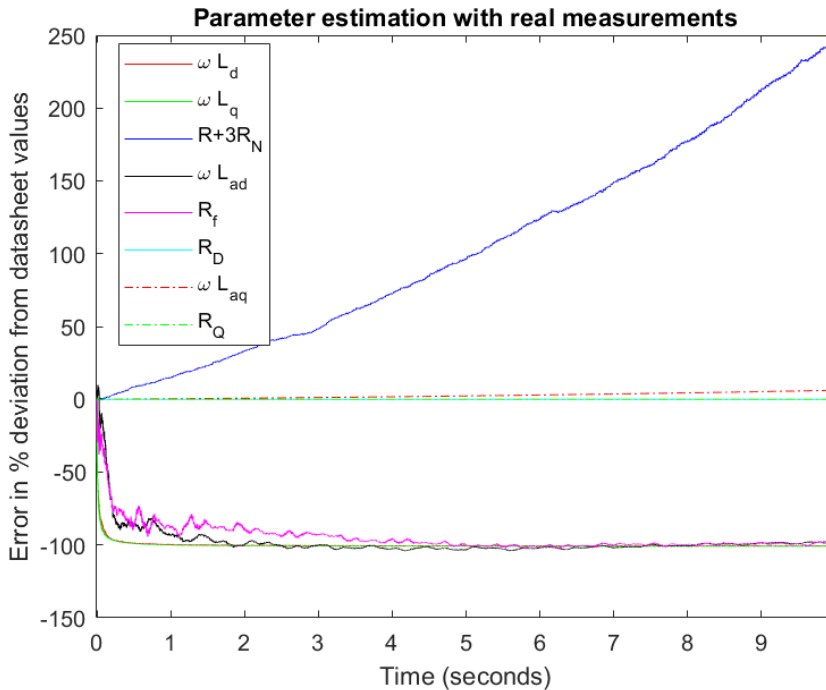


Figure 4.4: First ten seconds of error in parameter estimations from the RLS-block of estimating the parameters of the synchronous generator using data from real measurements while damper winding currents set to zero.

Figure 4.4 shows how the algorithm fastly gets unstable, and the error for the estimation of $R + 3R_N$ grows approximately exponentially and diverge. As shown in eq. (3.17), the parameter $R + 3R_N$ is estimated from by the zero-sequence current and voltage, i_0 and v_0 , respectively. The instability in the parameter estimation can be caused by rounding errors in the RLS algorithm, which is generally the main cause of instability of the algorithm. The rounding errors are caused by the errors being summed over time and then causing rapid growth of error [36]. Therefore, if the estimations from the Kalman Filter of i_0 and v_0 are affected by noise, the algorithm can get unstable and then diverge as $t \rightarrow \infty$. h

The other parameters, except the damper winding resistances, had large, but even deviations. The estimations quickly deviated from the initial conditions and stabilized with a deviation of about 100%. The small error in estimations of the damper windings resistance is not caused by a good estimate, but rather that the estimations are not updated from the $\hat{\theta}_0$ as the damper winding current is manually set to zero.

The percentage deviation in the estimated parameters from the RLS algorithm after the same simulation has run for 30 seconds is presented in table 4.4.

Table 4.4: Error deviation given in % from datasheet values for the parameter estimation from RLS after 30 seconds of simulation. Data from real measurements from generator during rated load, and damper winding currents set to zero.

Electrical parameter	Error in % deviation from actual value
$R_s + 3R_N$	25010
R_f	-102.32
L_{ad}	-103.23
L_{aq}	711.42
R_D	0.002
R_Q	0.002
X_d	-100.78
X_q	-101.13

Table 4.4 shows that the percentage error in the $R_s + 3R_N$ estimate continued to grow and shows no sign of converging. The error in the L_{aq} -estimate also showed tendencies to diverge as it continued to grow during the 30 seconds of simulation. The other estimations, except for damper winding resistances, stabilized at a error of about -100% early in the simulation, which can also be observed by table 4.4.

Additionally, estimations of the standard parameters are calculated by using eq. (2.25)-(2.34) and the estimated parameters from RLS. The estimations of the standard parameters are calculated by using eq. (2.25)-(2.34). The RLS-blocks estimates the parameters given in the R_{sm} matrix. However, there are more parameters which are included in the equations than these. Only four out of the eight parameters in the L_{sm} -matrix is estimated. The standard parameters are calculated by using estimated parameters for the ones included in R_{sm} and 'true' values for the others.

Table 4.5: Estimations of Standard Parameters given in % from datasheet values. Calculated from the estimated parameters from RLS, after 30 seconds of simulations, using measurements from real generator during rated load with damper winding currents assumed zero.

Standard parameter	Error in % deviation from datasheet value from datasheet value
X_d	100.78
X'_d	80.58
X''_d	79.789
T'_{do}	1125.7
T''_{do}	11.386
T'_d	3090
T''_d	7.7768
X_q	101.13
X''_q	152.14
T''_{q0}	171.49

Table 4.5 shows that none of the standard parameters is estimated satisfactory, and they all have large deviations from the datasheet values. Besides, when the damper winding currents are set to zero, only five of the parameters included in the equations for the standard parameters are estimated. The other parameters, L_{fd} , L_{1d} , L_{1q} , R_{1d} , R_{1q} , are not estimated and the 'true' value was used so that the standard parameters could be calculated.

4.3 Back to the "Synchronous Machine"-block

As the data proved to be unsatisfactory and the filtering was not as successful as hoped, it was decided it was pointless to continue forward with the same measurements. A goal of this master thesis was to perform a sensitivity analysis on the RLS algorithm to find out how sensitive it was to changes in the parameters. For example, it would be beneficial to know how the algorithm reacted if the mutual inductance deviated from its datasheet value. A sensitivity analysis would be pointless to perform on the measurements as it would be impossible to evaluate the results.

For this reason, it was decided to go back to the previous Simulink model used in [6] and [5]: Here, the measurements of v_{abc} , i_{abc} , u_f , and i_f is generated by a synchronous machine from the SPS library connected to an RL-load. The RLS-algorithm needs an initial estimation for the parameter, $\hat{\theta}_0$ as a starting point for the algorithm. In [6], [5], and, in addition, previously in this thesis, $\hat{\theta}_0$, was chosen equal to the true value of the parameter itself, θ . This is an unrealistic scenario, as in reality, the value of θ is unknown,

or else there would be no need to try to estimate it. It would, therefore, be interesting to explore how depended the RLS algorithm is on the value of $\hat{\theta}_0$, and if $\hat{\theta}$ would converge towards θ even if $\hat{\theta}_0$ deviated from θ . The sensitivity analysis was performed by changing the value of $\hat{\theta}_0$ away from θ . After this, the error between $\hat{\theta}$ and θ was evaluated. By this analysis, it can see how much the parameter estimation algorithm relies on the measurements versus the initial condition. The sensitivity analysis was performed by having $\hat{\theta}_0$ deviate ± 5 and 10% from θ .

The parameters estimated by the RLS algorithm are the ones present in the \mathbf{R}_{sm} matrix, and the standard parameter is recalculated by the use of these estimations. As the sensitivity analysis focuses on the RLS algorithm, and not the filtering and Kalman filter, all the simulations were performed without the addition of noise to the measurements from the synchronous machine model. Zero noise is not realistic, as there will always be noise present in the measurements from a machine. However, as the performance of the RLS algorithm is to be evaluated, it was decided that it would be easier to analyze the results without the presence of noise.

4.3.1 Sensitivity analysis

The simulations were performed using the same Simulink model that is presented in fig. 3.1. However, instead of the real measurements, the measurements were provided by a "synchronous machine"-block from the SPS library. The synchronous machine from Simulink was modelled to be equal to the generator presented previously in this chapter, in table 4.1. The RL-load connected to the machine was equal to the specified rated load. The simulations run for 60 seconds, to let the RLS algorithm converge to a value before the error in the parameter estimation was calculated. The simulations were all performed in the same manner, but with different values for the initial parameter estimation, $\hat{\theta}_0$. In this section five cases are presented for different values of $\hat{\theta}_0$, and the specification for the cases are listed below.

1. Case 1: Basecase: $\hat{\theta}_0 = \theta$
2. Case 2: - 5% deviation: $\hat{\theta}_0 = 0.95 \theta$
3. Case 3: 5% deviation: $\hat{\theta}_0 = 0.95 \theta$
4. Case 4: -10 % deviation: $\hat{\theta}_0 = 0.9 \theta$
5. Case 5: 10 % deviation: $\hat{\theta}_0 = 1.1 \theta$

4.3.1.1 Case 1: Basecase: $\hat{\theta}_0 = \theta$

The first scenario is the basecase, where the RLS-estimator was given the true value of the parameter as the initial condition. This case is used to validate the performance of the algorithm, and to have a reference for other cases. The results of the errors from the parameter estimation for this case is presented in fig. 4.5.

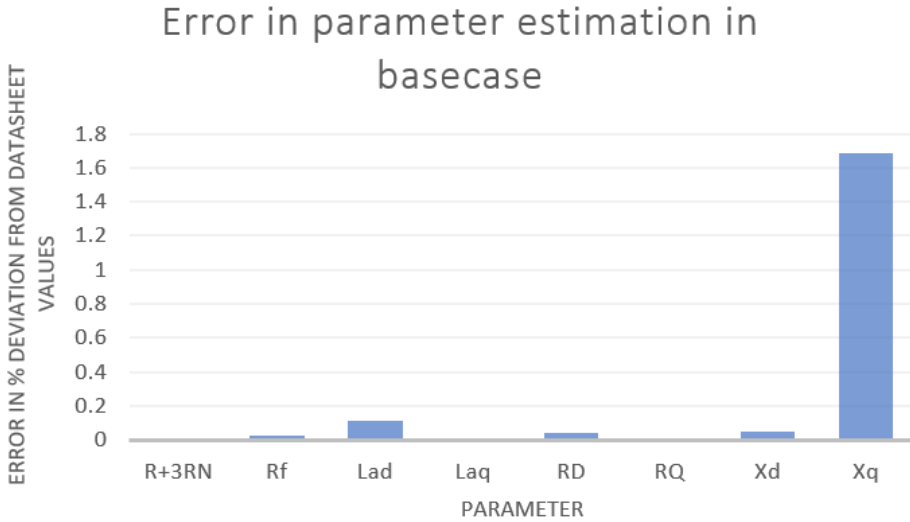


Figure 4.5: Errors of the parameter estimation for the basecase with $\hat{\theta}_0 = \theta$ in the RLS algorithm. Measurements from "Synchronous Machine"-block running on rated load during steady-state.

Table 4.6 shows the errors in the standard parameters calculated from the estimated parameters from the RLS algorithm.

Table 4.6: Error given in % of the estimated standard parameters compared to datasheet values. Standard parameters are calculated using the estimated parameters from the RLS-algorithm with $\hat{\theta}_0 = \theta$. Measurements from "Synchronous Machine"-block running on rated load during steady-state.

Standard parameter	Error deviation [%] from datasheet value
X_d	0.051674
X'_d	0.020095
X''_d	0.01851
T'_{do}	0.76181
T''_{do}	0.036554
T'_d	1.7592
T''_d	0.038139
X_q	1.6888
X''_q	0.00013111
T''_{q0}	0.0017783

Figure 4.5 shows that the RLS algorithm estimates the parameters of the machine with minimal percentage deviations, whose values are in line with those achieved in [6]. The standard parameters are also calculated from the estimated parameters and give very small errors, as can be seen in table 4.6.

4.3.1.2 Case 2: $\hat{\theta}_0 = 0.95 \theta$

The second case was performed in the same manner as the basecase, except the initial parameter value given to the RLS-estimator was chosen equal to 0.95θ . The errors from the parameter estimation is given in fig. 4.6 for the estimated parameters and in table 4.7 for the standard parameters.

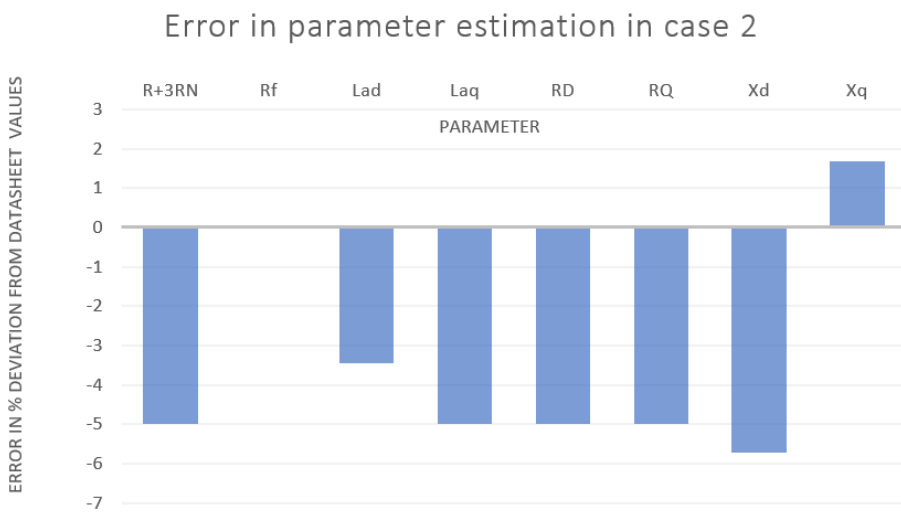


Figure 4.6: Errors of the parameter estimation for the basecase with $\hat{\theta}_0 = 0.95\theta$ in the RLS algorithm. Measurements from "Synchronous Machine"-block running on rated load during steady-state.

Table 4.7: Error given in % of the estimated standard parameters compared to datasheet values. Standard parameters are calculated using the estimated parameters from the RLS-algorithm with $\hat{\theta}_0 = 0.95 \theta$. Measurements from "Synchronous Machine"-block running on rated load during steady-state.

Standard parameter	Error deviation [%] from datasheet value
X_d	- 5.7287
X'_d	- 0.65332
X''_d	- 0.60212
T'_{do}	-1.7405
T''_{do}	5.2439
T'_d	1.6862
T''_d	5.2981
X_q	- 1.6922
X''_q	3.0874
T''_{q0}	3.8965

Figure 4.6 shows by giving the RLS-estimator an incorrect value for $\hat{\theta}_0$ this resulted in almost the same error in the estimation of the parameters. The exception is for R_f , which converged to its actual value. Table 4.7 shows that the errors in the calculated standard parameters was considerably increased compared to table 4.6.

4.3.1.3 Case 3: $\hat{\theta}_0 = 1.05 \theta$

The third case was performed with the initial parameter value equal to 5 % larger than the true value. The errors of the parameter estimation for this value of $\hat{\theta}_0$ in the RLS algorithm is presented in fig. 4.7. Also, the deviation in the calculated standard parameters compared to the datasheet values is listed in table 4.8.

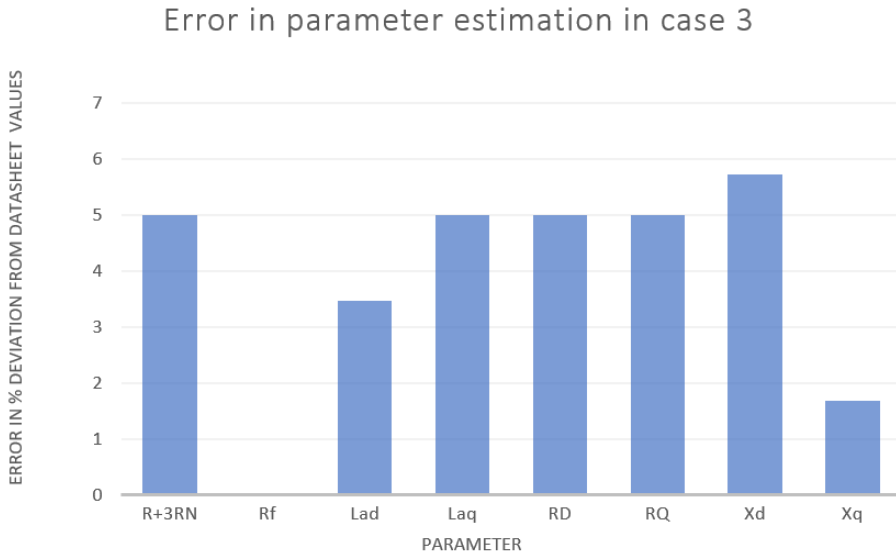


Figure 4.7: Errors of the parameter estimation for the basecase with $\hat{\theta}_0 = 1.05\theta$ in the RLS algorithm. Measurements from "Synchronous Machine"-block running on rated load during steady-state.

Table 4.8: Error given in % of the estimated standard parameters for Case 3: $\hat{\theta}_0 = 1.05\theta$

Standard parameter	Error deviation [%] from datasheet value
X_d	5.832
X'_d	0.58244
X''_d	0.53622
T'_{do}	3.2642
T''_{do}	4.6774
T'_d	1.828
T''_d	4.7212
X_q	1.6854
X''_q	3.0078
T''_{q0}	3.522

The interesting result can now be observed as fig. 4.7 and fig. 4.6 appears to be almost mirrored about the x-axis, as the results from the third case give the same deviation in parameter estimation but with switched signs. This is true except for the estimation for X_q , which had a consistent error in both cases, equal to the error in the basecase.

4.3.1.4 Case 4: $\hat{\theta}_0 = 0.90 \theta$

The fourth case was performed with $\hat{\theta}_0 = 0.90 \theta$, and the results from the parameter estimation is shown in fig. 4.8 and table 4.9.

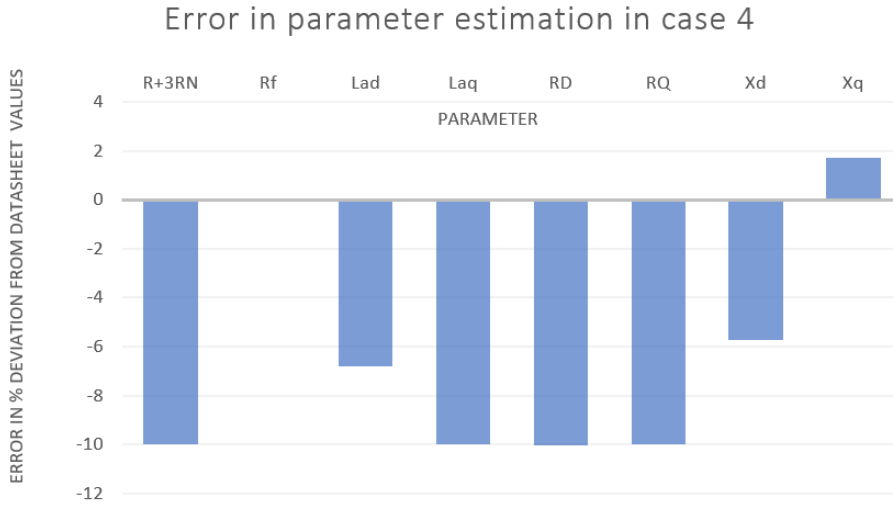


Figure 4.8: Errors of the parameter estimation for the case 4 with $\hat{\theta}_0 = 0.9\theta$ in the RLS algorithm. Measurements from "Synchronous Machine"-block running on rated load during steady-state.

Table 4.9: Error given in % of the estimated standard parameters for Case 4: $\hat{\theta}_0 = 0.9 \theta$

Standard parameter	Error deviation [%] from datasheet value
X_d	-11.509
X'_d	-1.3196
X''_d	-1.2169
T'_{do}	-4.2429
T''_{do}	11.027
T'_d	1.6084
T''_d	11.142
X_q	-1.6956
X''_q	6.257
T''_{q0}	8.224

Figure 4.8 shows how the error in the parameter estimation for $R + 3R_N$, L_{ad} , L_{aq} , R_D , R_Q and X_d increased as $\hat{\theta}_0$ deviated farther from the true value.

4.3.1.5 Case 5: $\hat{\theta}_0 = 1.1 \theta$

The fifth and last case was performed with $\hat{\theta}_0$ being 10% larger than the true value and the results are given in fig. 4.9 and table 4.10.

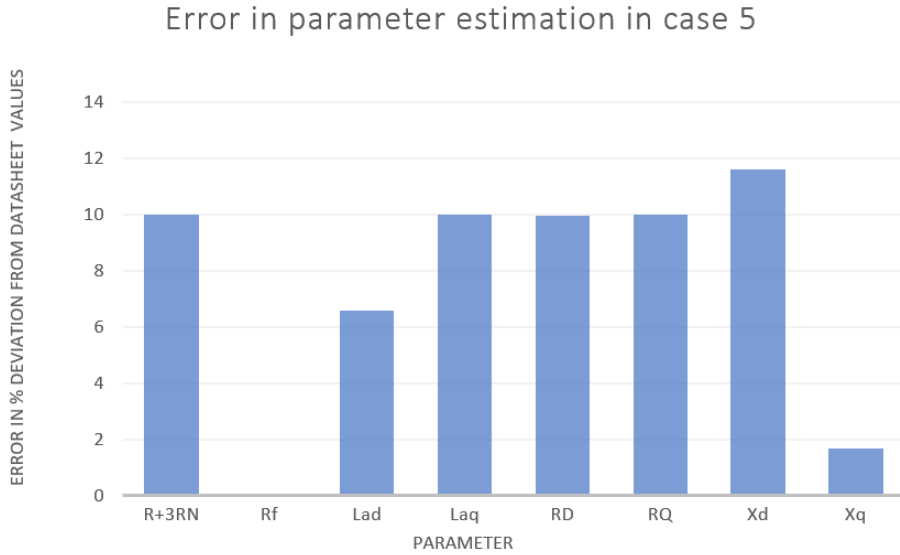


Figure 4.9: Errors of the parameter estimation for the case 4 with $\hat{\theta}_0 = 1.1\theta$ in the RLS algorithm. Measurements from "Synchronous Machine"-block running on rated load during steady-state.

Table 4.10: Error given in % of the estimated standard parameters for Case 5: $\hat{\theta}_0 = 1.1 \theta$

Standard parameter	Error deviation [%] from datasheet value
X_d	11.612
X'_d	1.1565
X''_d	1.1565
T'_{do}	5.7665
T''_{do}	8.9651
T'_d	1.8928
T''_d	9.0481
X_q	1.682
X''_q	5.9396
T''_{q0}	6.7255

Another interesting fact showed in the sensitivity analysis, is that the estimations for R_f and X_q seems to be largely insensitive to changes in $\hat{\theta}_0$, while the others showed deviations. The error for the estimations of R_f and X_q stayed in line with the ones presented

in the basecase.

4.4 Tuning of Algorithm

The results from the sensitivity analysis and the changing of $\hat{\theta}_0$ showed that an error between $\hat{\theta}_0$ and θ_0 produced the same error in the estimation of θ for most of the estimated parameters. The reason for this could be that the RLS-estimator trusted the initial parameter estimation too much and thereby not letting the new measurements update the estimation. This unfortunate tendency is desired to be corrected so that the RLS-estimator would converge to the correct value of θ . To correct this, the two other block inputs of the RLS-estimator block, namely λ and P_0 , was attempted to tune separately. The results after the tuning are presented in section 4.4.1 and section 4.4.2.

4.4.1 Tuning of Forgetting Factor, λ

There are multiple variables which affect the final value of the parameter estimation, but one important one is the forgetting factor. Due to the forgetting factor, older observations will have a smaller influence than newer ones. [31].

The forgetting factor is closely related to the *memory horizon* and this term is defined as:

$$T_\lambda = \frac{1}{1 - \lambda} = f_s T_m \quad (4.1)$$

As the memory horizon is a more physical term, it is convenient to write the forgetting factor as a function of the memory horizon:

$$\lambda = 1 - \frac{1}{f_s T_m} \quad (4.2)$$

The memory horizon was initially chosen to be 10 seconds, which gives a $\lambda = 0.998$. A larger memory horizon leads to a larger forgetting factor and vice versa. The smaller that λ is, the more sensitive the filter is to recent samples, as the previous samples have a smaller contribution to the covariance matrix. A $\lambda=1$ corresponds to infinite memory. The forgetting factor, λ is usually chosen between 0.98 and 1 [37].

An initial guess was that by reducing the memory horizon, the algorithm would rely less on the initial value and rely more on the measurements. It would thereby give more accurate estimation even with deviations in the initial values. There were performed several

rounds of simulation with different values for the memory horizon, but no improvement of the parameter estimation was achieved. It was however noticed that too small values for the memory horizon (shorter than 2 seconds) led to an unstable algorithm.

4.4.2 Tuning of the Initial Parameter Covariance Matrix

Another user input to the RLS-block is the initial value for the parameter covariance matrix, \mathbf{P}_0 . The value \mathbf{P}_0 is chosen based on the knowledge of the parameters at the starting time. If the knowledge is vague, a high value is to be expected.

The choice of the initial values is paramount in the real-life application of RLS schemes. If \mathbf{P}_0 is small, the value will not change much from the initial values, but if \mathbf{P}_0 is large, the next estimation will quickly jump away from the initial value. Without prior knowledge, it is common knowledge to choose \mathbf{P}_0 to a 'large number' [29].

The value for \mathbf{P}_0 was initially chosen to be 0.05, and equal for all RLS-blocks. The value of \mathbf{P}_0 will not be equal for all machines and should be adjusted according to the knowledge of the parameters. For this reason, it is also natural to increase the values of \mathbf{P}_0 as the knowledge of the parameters is decreased, when the value of $\hat{\theta}_0$ deviated far from θ_0 .

The value for \mathbf{P}_0 was tuned in an ad-hoc manner, were $\hat{\theta}_0$ had a +10% deviation from the true value. It was quickly observed that a larger value of \mathbf{P}_0 decreased the error in the parameter estimation, bringing the estimated value closer the actual value. It was thereby showed that the RLS algorithm depended less on the initial value. It was also observed that a too large value for \mathbf{P}_0 gave a too large jump in the parameter estimation, and caused instability.

The best result was achieved with $\mathbf{P}_0 = 25$, a value hundred times larger than the original value used in [6] and [5]. The error from the parameter estimation and the estimation of the standard parameters are shown in fig. 4.10 and table 4.9.

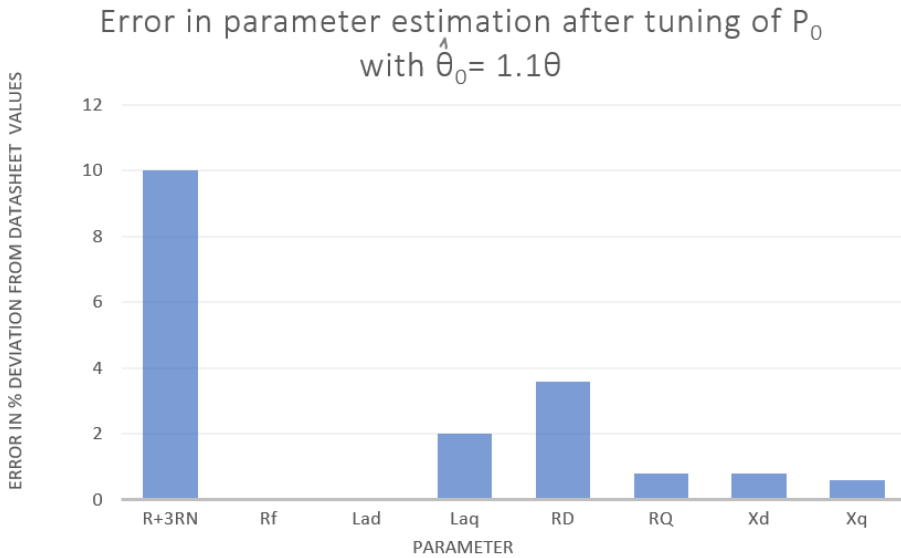


Figure 4.10: Errors of the parameter estimation after tuning P_0 with $\hat{\theta}_0 = 1.1\theta$ in the RLS algorithm. Measurements from "Synchronous Machine"-block running on rated load during steady-state.

Table 4.11: Standard Parameter estimation with 10% larger parameters.

Standard parameter	Error deviation [%] from datasheet value
X_d	0.81826
X'_d	0.81826
X''_d	0.05962
T'_{do}	1.0934
T''_{do}	2.839
T'_d	1.7555
T''_d	5.833
X_q	0.5908
X''_q	1.7396
T''_{q0}	1.7067

The comparison of fig. 4.10 and 4.9 to fig. 4.9 and 4.10, respectively, shows that with a larger value of of P_0 , the error in the parameter estimation has significantly decreased for all values except $R + 3R_N$. There attempted to change the value of P_0 for this RLS-block independently, but the estimation did not improve.

Figure 4.11 highlights how the algorithm manages to converge the estimate to the correct value even with an initial error of 10%, illustrated with the estimation for the parameter, L_{ad} .

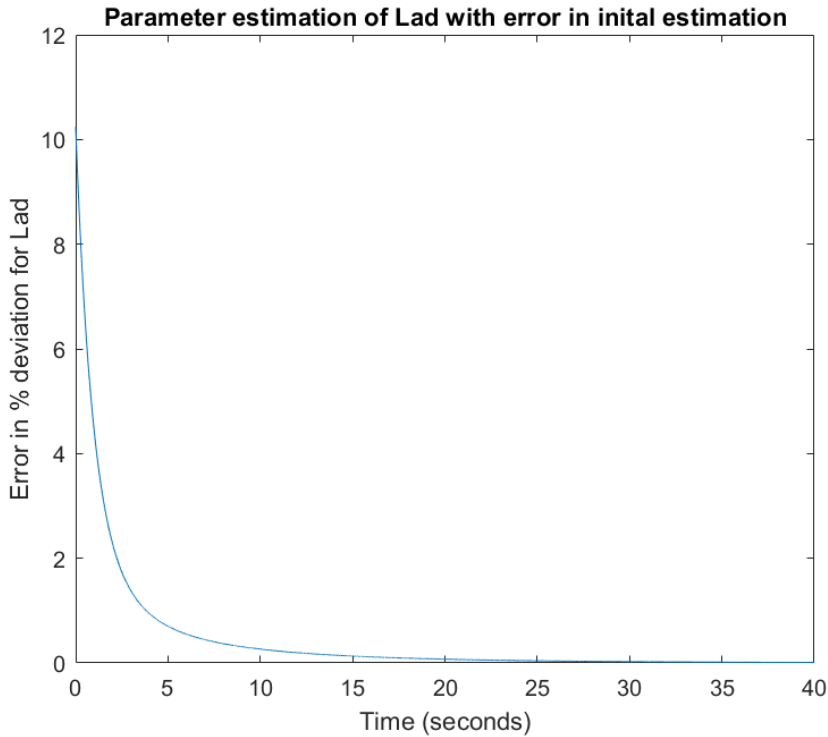


Figure 4.11: Errors of the parameter estimation of L_{ad} after tuning P_0 with $\hat{\theta}_0 = 1.1\theta$ in the RLS algorithm. Measurements from "Synchronous Machine"-block running on rated load during steady-state.

Figure 4.11 shows how the parameter estimation of the mutual inductance on the d-axis, L_{ad} , starts with an initial error of 10%, but after about 25 seconds this error is approximately zero without any overshoot. The rise time of the estimation is 3.6 seconds, where the rise time is specified as the time the algorithm has gone from a 9% to a 1% error in the estimation.

Discussion

5.1 Results using real data

The main goal of this master thesis was to validate the parameter estimation model created in [6] with measurements collected from real a real power plant. The concept of the algorithm is to use these measurements to improve upon manufacturers parameter estimation for synchronous machine parameters. Early simulations of the algorithm, presented in section 4.2, by using data from a real generator, however, revealed large amounts of noise present in the measurements of the field voltage and currents. The noise-corrupted data resulted in extremely poor parameter estimation. There was made several attempts of trying to filter out the noise, but in fear of wasting too much time and with the risk of not achieving good results from filtering, the measurements were put aside. Filter design was out of the scope of the thesis, and filtering techniques were initially not thoroughly investigated. There could be ways to design a filter which made the measurements useful for testing of the algorithm, even as this was not achieved in this thesis.

The main disadvantage of the RLS is the fact that the noise model, for which unbiased estimates are obtained, is very unrealistic in practical situations since, in general, the disturbance is not just white. [26]

The noisy measurements, however, reveal the problem of the algorithm not being able to handle non-white noise. In [6] it was proved that the algorithm could handle white band-limited noise, but real measurements often include noise which is not perfectly white. In

general, generating stations are well known for poor electromagnetic interference environment [25], but the results suggested that the estimator accuracy could be improved by the designing of effective filters. A possible extension of the algorithm would, therefore, be to handle a larger selection of noise. Besides, it would be helpful if the algorithm could detect and reject bad measurements, such as the reliability of the results would be improved.

5.1.1 Leakage inductance

Another thing which can be discussed which was briefly mentioned previously is the subject of the leakage inductance. When calculating the parameters of the machine used in this thesis, the actual value for the leakage inductance was used. However, there are not many instances where the knowledge of the synchronous generator is as great as in this thesis, and the leakage inductance is often unknown. If it is not known, it has to be estimated together with the other parameters, which adds more uncertainty to parameter estimation.

5.2 Sensitivity analysis

The sensitivity analysis performed in section 4.3.1 presented the problem of the algorithm seemed to rely too much on the input of the initial estimate for the parameter, namely $\hat{\theta}_0$. All the four cases gave the same result of a deviation in $\hat{\theta}_0$ from the true value almost exclusively resulted in the same error in the parameter estimation. The reason for this is suspected to be a poorly tuned RLS algorithm for this specific machine, and this assumption is proved to be correct as the tuning of the P_0 later showed good improvement in the parameter estimation. As the algorithm showed that it would converge towards correct value of θ even with errors in $\hat{\theta}_0$, this implies that the algorithm could be able to detect faults within few seconds. Therefore, the continuous tracking of the parameter values could give the companies the opportunity to foresee generator failures and possibly avoid outages.

5.2.1 Tuning of algorithm

The results in section 4.4.2 shows that the parameter estimation considerably improved by the tuning of the initial parameter covariance matrix. There is good reason to believe that by continuous tuning, a better value could be found. Also, the values for \mathbf{P}_0 should possibly have been tuned separately to find the optimal value. Additionally, there exist

more convenient and methodical ways of tuning the algorithm, as the tuning-method was quite time-consuming.

There was, also suspected that tuning of the forgetting factor would have improved upon the estimation, but this effect was not achieved. The reasons for this is not straight forward, but can be due to a couple of reasons; One being that the forgetting factor remained constant through the entirety of the estimation, and other that; λ and P_0 were tuned independently. The idea to adjust λ has been proposed in [38], and in [39] showed how a way for the forgetting factor to be selected optimally and that this resulted in an algorithm which was less sensitive to noise while the tracking ability was well retained. There is also a possibility that the tuning of λ in combination with the tuning of P_0 would have given favourable results.

A problem with the tuning of the algorithm for each machine is that it is much easier to perform the tuning of the algorithm when the correct value of the parameter is known. This way, the performance of the algorithm could always be evaluated, and the tuning could be performed until a satisfactory result for the parameter estimation was received. This is often not the case, as when performing the parameter estimation on an actual machine, the true value is not known, and if it were, there would be no point for the parameter estimation. When the true values of the parameters of the machine at an operating point are unknown, so it is not possible to derive any definite conclusions about the accuracy of the estimation. This fact also makes it hard to verify the algorithm, as the percentage deviations from the manufacturer's values of the parameters cannot be used to validate or reject the proposed method.

The parameter estimation algorithm in total has a lot of complexity. In total, there is plenty of parameters which should be tuned, from the multiple parameters in the Kalman Filter to the RLS algorithm. Besides, to receive a good parameter estimation, a great deal of knowledge has to be known about the system, both the algorithm and the machine itself. Even though the extensive tuning of the algorithm for each machine could be cumbersome, from section 4.4.2, there is reason to believe that good tuning can give good estimations even if the knowledge about the parameters is not perfect.

Conclusion and Future Work

6.1 Summary and Conclusion

The focus for this master thesis was to continue the work performed this last fall in [5] and the master thesis of Erick F.Alves in [6], on the online parameter estimation of synchronous machines. A natural continuation of the previous work was to modify the model to validate the algorithm using current and voltage measurements from a real synchronous generator available without taking the machine out of service. The data used to test the algorithm was from a ten pole salient-pole synchronous generator from Voith situated in a German hydropower-plant. Naturally, the first step was to use the rated data of the machine in addition to the standard parameters from the datasheet to define the resistances and inductances to be able to create an accurate model of the machine. The electrical parameters were calculated using the equations presented in [23]. A good part of the effort in this thesis was put into understanding the equations and parameters of the synchronous generator, where the pu system, not surprisingly, proved to be a very confusing element of this. After all the per-unit values for the generator was calculated, the state-space equations for the machine could be created according to eq. (3.3). The next step was to create the Simulink model, which uses the current and voltage measurements to create an estimate for the machine parameters. No measurements of the rotor position, so the angle was estimated using a phase-locked-loop Controller, or a PLL. The parameter estimation was performed by using a Kalman filter for noise filtering and the Recursive Least Square algorithm to each estimate the parameters: $R + 3R_N$, R_f , R_D , R_Q , X_d ,

X_q , L_{ad} , and L_{aq} .

However, one significant problem stopped the validation of the algorithm using real data, and that was the presence of large amounts of nonwhite noise in the measurements of the field current and voltage. There was attempted several methods for filtering the measurements, but all proved to be unsatisfactory. The results from the parameter estimation using the noisy measurements gave large deviations compared to the datasheet values. As the noisy measurements lead to high oscillations in the observation of the damper winding currents, the parameter estimation was also performed by setting the damper winding currents to zero in the model. However, this led to instability of the RLS algorithm for both $R + 3R_N$ and L_{aq} . The algorithm did not give a good estimation for any of the other parameters either.

Another goal of the master thesis was to perform a sensitivity analysis of the estimation model and the RLS to find out how the algorithm reacted to changes in the machine parameters. As the measurements from the real generator proved to be unsatisfactory, it was decided to rather use measurements generated by a "Synchronous Machine"-block in the Simulink library. The sensitivity analysis was performed by introducing an error of $\pm 5\%$ 10% to the initial parameter estimation, $\hat{\theta}_0$, in the RLS-algorithm, and then evaluating if the estimation is able to converge to the true value. The initial results of the sensitivity analysis showed that an initial error in $\hat{\theta}_0$ gave the same error in θ for $R + 3R_N$, R_D , R_Q , X_d , L_{ad} , and L_{aq} . The reasons for this was concluded to be poor tuning of the RLS-algorithm, making the estimator trusting the initial estimation too much and not updating the estimation with new observations from the measurements.

The next step was to attempt to tune the algorithm by tuning the forgetting factor, λ , and the initial parameter covariance matrix, P_0 . The tuning of the forgetting factor showed no improvements in the parameter estimation as initially suspected, but it was experienced that a too small value for the factor resulted in instability. However, the tuning of the initial parameter covariance matrix, P_0 , led to more success. The best result was achieved with a P_0 equal to 25, which was 100 times higher than the value used for the simulations in section 4.3.1. After the tuning, a better estimation was achieved for all parameters except $R + 3R_N$. The improvement in the parameter estimation caused by tuning P_0 comes from its definition. P_0 is to be chosen based on how good the initial estimation for the parameter is, so when the $\hat{\theta}_0$ deviated largely from θ , the RLS-algorithm this value should be increased accordingly. There is also reasons to believe that the parameter estimations could be further improved from the results in section 4.4.2 by a more methodical tuning.

6.2 Future Work

- The algorithm is still not able to perform the parameter estimation on a synchronous generator in real time. A more sophisticated method for testing the algorithm would be to program the algorithm by using an object-oriented GUI, to be able to receive measurements directly from the generator, which is done in [25]. By using this approach, the algorithm would be able to run in real-time, and from there be used for fault detection and investigating issues of stability and robustness.
- Actually test the algorithm on data from real power plant. Preferably multiple to be able to validate the method.
- Expand the model to handle the nonlinearity of the synchronous machine such that the parameters of L_{sm} which are included in the equations for the standard parameters also could be estimated.

Bibliography

- [1] James R. Bumby Jan Machowski, Janusz W. Bialek. *Power System Dynamics, Stability and Control*. John Wiley and Sons, Ltd, 2008.
- [2] NVE. Vannkraft. <https://www.nve.no/energiforsyning/vannkraft/>, Nov. 2019. Accessed on 12/12/19.
- [3] G. Valverde, E. Kyriakides, G. T. Heydt, and V. Terzija. Nonlinear estimation of synchronous machine parameters using operating data. *IEEE Transactions on Energy Conversion*, 26(3):831–839, Sep. 2011.
- [4] E. Ghahremani, M. Karrari, M. B. Menhaj, and O. P. Malik. Rotor angle estimation of synchronous generator from online measurement. In *2008 43rd International Universities Power Engineering Conference*, pages 1–5, 2008.
- [5] Sophie S. Berg. Project thesis: Real-time parameter identification for reliable operation of synchronous generators. 2019.
- [6] Erick F. Alves. Master’s thesis: Reliable parameter identification for synchronous machines. Master’s thesis, UiT, Department of Electrical Engineering, 2018.
- [7] S. H. Wright. Determination of synchronous machine constants by test reactances, resistances, and time constants. *Transactions of the American Institute of Electrical Engineers*, 50(4):1331–1350, 1931.
- [8] H. Agahi, M. Karrari, W. Rosehart, and O. P. Malik. Application of active identification method to synchronous generator parameter estimation. In *2006 IEEE Power Engineering Society General Meeting*, pages 7 pp.–, 2006.

-
- [9] R. H. Park. Two-reaction theory of synchronous machines generalized method of analysis-part i. *Transactions of the American Institute of Electrical Engineers*, 48(3):716–727, July 1929.
- [10] Giancarlo Marafiotto Erick F. Alves, Jonas K. Nøland and Geir Mathisen. Online parameter identification of synchronous machines using kalman filter and recursive least squares. 2019.
- [11] M. Dehghani Z. Gallehdari and S. K. Y. Nikraves. Online state space model parameter estimation in synchronous machines. *Iranian Journal of Electrical Electronic Engineering*, 10, 2014.
- [12] E. Eitelberg and R. G. Harley. Estimating synchronous machine electrical parameters from frequency response tests. *IEEE Transactions on Energy Conversion*, EC-2(1):132–138, March 1987.
- [13] E. Kyriakides, G. T. Heydt, and V. Vittal. Online parameter estimation of round rotor synchronous generators including magnetic saturation. *IEEE Transactions on Energy Conversion*, 20(3):529–537, Sep. 2005.
- [14] Chi Choon Lee. *Synchronous Machine Modeling by Parameter Estimation*. Louisiana State University, 1976.
- [15] A. Keyhani and S. I. Moon. Maximum likelihood estimation of synchronous machine parameters and study of noise effect from dc flux decay data. *IEE Proceedings C - Generation, Transmission and Distribution*, 139(1):76–80, Jan 1992.
- [16] H. Tsai, A. Keyhani, J. Demcko, and R. G. Farmer. On-line synchronous machine parameter estimation from small disturbance operating data. *IEEE Transactions on Energy Conversion*, 10(1):25–36, March 1995.
- [17] K. Rao. *Wind Energy for Power Generation: Meeting the Challenge of Practical Implementation*. 01 2019.
- [18] Hadi Saadat. *Power System Analysis*. PSA Publishing, 3rd edition, 2010.
- [19] R. E. Doherty and C. A. Nickle. Synchronous machines i — an extension of blondel’s two-reaction theory. *Journal of the A.I.E.E.*, 45(10):974–987, 1926.
- [20] L. Dreyfus. Ausgleichvorgänge beim plotzlichen kurzschluss von synchron generatoren. *Electrotech*, 1916.

-
- [21] P. L. Dandeno, P. Kundur, and R. P. Schulz. Recent trends and progress in synchronous machine modeling in the electric utility industry. *Proceedings of the IEEE*, 62(7):941–950, July 1974.
- [22] Charles Concordia. *Synchronous machines : theory and performance*. John Wiley and Sons, Inc., 1951.
- [23] P. Kundur. *Power System Stability and Control*. McGraw-Hill, 1994.
- [24] P.M Anderson and A.A Fouad. *Power System Control and Stability*. John Wiley and Sons, Inc., 2nd edition, 2003.
- [25] G.Karady K.Holbert S.Borkar W.Gu V.Vittal G.Huang K.Men G.Heydt, E.Kyriakides. Estimation of synchronous generator parameters from on-line measurements. 2005.
- [26] P.S.R. Diniz. *Adaptive Filtering*. Springer AS, 2008.
- [27] R.E. Kalman. A new approach to linear filtering and prediction problems. 1960.
- [28] Robert G. Brown and Patrick Y.C Hwang. Introduction to random signals and applied kalman filtering, 4th edition. 2012.
- [29] Kristiaan Pelckmans. System identification. <https://www.it.uu.se/edu/course/homepage/systemid/vt12>, 2012. Accessed on 05/28/20.
- [30] Sergey Borodachev. Recursive least squares method of regression coefficients estimation as a special case of kalman filter. volume 1738, page 110013, 06 2016.
- [31] Lennart Ljung. Recursive identification algorithms. <http://www.control.isy.liu.se/research/reports/2001/2366.pdf>, 2001. Accessed on 04/12/19.
- [32] C. Paleologu, J. Benesty, and S. Ciochină. A practical variable forgetting factor recursive least-squares algorithm. In *2014 11th International Symposium on Electronics and Telecommunications (ISETC)*, pages 1–4, 2014.
- [33] Peter C. Young. *Recursive Estimation and Time-Series Analysis*. Springer, 2nd edition, 2011.
- [34] X. Chen, X. Zha, and C. Li. Design of a damper winding currents observer of twelve-phase synchronous generator for parameters identification. In *2010 Asia-Pacific Power and Energy Engineering Conference*, pages 1–4, March 2010.

-
- [35] Mathworks. Recursive least squares estimator. <https://www.mathworks.com/help/ident/ref/recursiveleastsquaresestimator.html>. Accessed on 04/12/19.
- [36] Richard J. Duro and López Fernando Peña. *Digital Image and Signal Processing for Measurement Systems*. River Publishers, 2012.
- [37] Emmanuel C. Ifeachor, Barrie W. Jervis, Erik L. Dagless, and Joann O'Reilly. *Digital signal processing: A practical approach*. 1993.
- [38] T. Hägglund. The problem of forgetting old data in recursive estimation. pages 213–214, 1984.
- [39] W.K. Yung and K.F. Man. Optimal selected forgetting factor for rls estimation. *IFAC Proceedings Volumes*, 26(1):331–334, Optimal Selected Forgetting Factor for RLS Estimation.

